

Journal Pre-proofs

Butyl methyl imidazolium silica sulfate (BMIm)SS: A novel hybrid nano-catalyst for highly efficient synthesis of new 1,2-diol monoesters of ibuprofen as the novel prodrugs of ibuprofen having potent analgesic property

Mohammad Navid Soltani Rad, Somayeh Behrouz, Esmaeil Atashbaste, Seyedeh-Sara Hashemi

PII: S0045-2068(20)31868-X
DOI: <https://doi.org/10.1016/j.bioorg.2020.104570>
Reference: YBIOO 104570

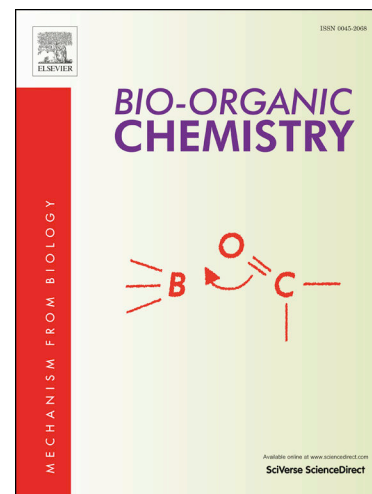
To appear in: *Bioorganic Chemistry*

Received Date: 9 October 2020
Revised Date: 4 December 2020
Accepted Date: 16 December 2020

Please cite this article as: M. Navid Soltani Rad, S. Behrouz, E. Atashbaste, S-S. Hashemi, Butyl methyl imidazolium silica sulfate (BMIm)SS: A novel hybrid nano-catalyst for highly efficient synthesis of new 1,2-diol monoesters of ibuprofen as the novel prodrugs of ibuprofen having potent analgesic property, *Bioorganic Chemistry* (2020), doi: <https://doi.org/10.1016/j.bioorg.2020.104570>

This is a PDF file of an article that has undergone enhancements after acceptance, such as the addition of a cover page and metadata, and formatting for readability, but it is not yet the definitive version of record. This version will undergo additional copyediting, typesetting and review before it is published in its final form, but we are providing this version to give early visibility of the article. Please note that, during the production process, errors may be discovered which could affect the content, and all legal disclaimers that apply to the journal pertain.

© 2020 Elsevier Inc. All rights reserved.



Butyl methyl imidazolium silica sulfate (BMIm)SS: A novel hybrid nano-catalyst for high **ovel** prodrugs of ibuprofen having potent analgesic property

Journal Pre-proofs

Mohammad Navid Soltani Rad,^{a*} Somayeh Behrouz,^{a*} Esmaeil Atashbaste^a Seyedeh-Sara Hashemi^b

^a Medicinal Chemistry Research Laboratory, Department of Chemistry, Shiraz University of Technology, Shiraz 71555-313, Iran

^b Burn and Wound Healing Research Center, Division of Food and Nutrition, Shiraz University of Medical Sciences, Shiraz, Iran

Abbreviations: IBP, ibuprofen; [BMIm]SS, butyl methyl imidazolium silica sulfate; NSAIDs, nonsteroidal anti-inflammatory drugs; COX, cyclooxygenase; SSA, silica sulfuric acid; OIHs, organic-inorganic hybrid catalysts; PGs, prostaglandins; GI, gastrointestinal; ILs, ionic liquids; SILs, supported ionic liquids; [BMIm]Br, butyl methyl imidazolium bromide; [BMIm]OH, butyl methyl imidazolium hydroxide; XRD, X-ray diffraction; SEM, scanning electron microscopy; EDS, Energy-dispersive X-ray spectroscopy; TGA, thermogravimetric analysis, MVD, Molegro Virtual Docker; RMSD, root-mean-square deviation; Lipinski's RO5, Lipinski's rule of 5; nHba, number of hydrogen bond acceptors; nHbd, number of hydrogen bond donors; nrotb, number of rotatable bonds; TPSA, total polar surface area

*Corresponding authors. Tel.: +98 71 3735 4500; Fax: +98 71 3735 4520; *E-mail address:* soltani@sutech.ac.ir (M.N. Soltani Rad); behrouz@sutech.ac.ir (S. Behrouz)

Abstract:

The fabrication, characterization of butyl methyl imidazolium silica sulfate [BMIm]SS as a novel nano hybrid catalyst and its application in synthesis of new ibuprofen (IBP) 1,2-diol mono esters were described. [BMIm]SS catalyzed the reaction of IBP with epoxides to afford the new IBP 1,2-diol mono esters in good to excellent yields. The products were tested *in vivo* for the analgesic properties on female mice using formalin test. The test results revealed that most compounds, in particular compounds **1h**, **1k** and **1o** displayed potent analgesic activity compare to IBP as a reference drug. No mortality was observed due to the toxicity of the synthesized compounds. The docking analysis was conducted that confirmed the strong binding affinity of active compounds to active site of murine cyclooxygenase-2 (COX-2) enzyme compare to IBP. The *in silico* pharmacokinetic profile, drug likeness and toxicity predictions were carried out for all compounds which determined that **1h** can be suggested as an appropriate future drug candidate.

Keywords: *Ibuprofen, 1,2-diol monoesters, [BMIm]SS, analgesic, formalin test, NSAIDs, cyclooxygenase.*

1. Introduction

Nonsteroidal anti-inflammatory drugs (NSAIDs) are a broad heterogeneous group of compounds that have been immensely used for decades as highly efficient analgesic [1]. NSAIDs are among the most frequently used therapeutic agents not only by issue but also many of them are present over-the-counter allowing for self-medication [2]. They are medicated for numerous diseases, including arthritis, osteoarthritis and musculoskeletal disorders [3]. While most of the biological activities of NSAIDs are associated with COX-dependent mechanisms; however, several studies have evidenced that NSAIDs interact with membrane phospholipids in a COX-independent route that could be involved in their biological activity [4-13]. Structurally, NSAIDs are categorized to salicylates, sulfonanilides, coxibs, propionic, acetic, enolic and anthranilic acids derivatives [14]. The structures of some popular NSAIDs are shown in Fig. 1[15].

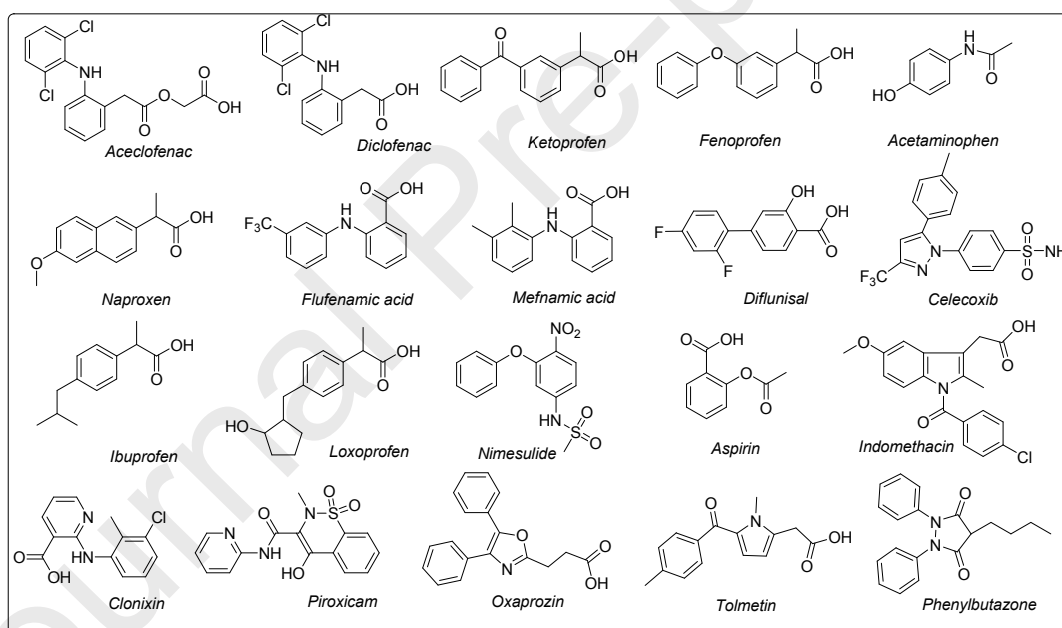


Fig.1. Structure of some NSAIDs from diverse categories.

Ibuprofen (IBP), (R, S) [2-(4-isobutylphenyl) propionic acid] was the first NSAID belongs to category of propionic acid derivatives that universally used for the therapy of pain and inflammation [16]. It is one of the strongest orally and highly active NSAID that widely used in the treatment of osteoarthritis, rheumatoid arthritis, muscle pain and recent surgery [17, 18]. Like most NSAIDs, IBP blocks cyclooxygenase (COX) enzyme and inhibits prostaglandins (PGs) biosynthesis [19]. In spite of its remarkable pharmaceutical benefits; however, IBP involves unwanted side effects in particular on

human digestion system. Progress in the gastrointestinal (GI) side effects especially stomach ulceration, bleeding and perforation are the main limitations in its oral administration which is especially due to local action exerted by direct contact of drug with gastric mucosa [20]. In this context, the free carboxylic acid moiety in IBP structure plays an important role in maintaining and magnifying the disorders caused by stomach ulcers [21]. Thus, it is critically essential to convert IBP into relevant prodrugs. Up to date, diverse drugs, molecules and carriers were used to conjugate with IBP for different purposes like preparation of mutual prodrugs of IBP, variation in blood-brain barrier and alteration in pharmacokinetic profiles of IBP [22]. For instance, IBP has been conjugated with sulfa drugs (**I**) [23], eugenol (**II**) [24], menthol (**III**) [25], thymol (**IV**) [25], chlorzoxazone (**V**) [26], acetaminophen (**VI**) [27], medoxomil (**VII**) [28], guaiacol (**VIII**) [29], N-hydroxy-methylphthalimide (**IX**) [30], hydroxy ethylsulfohydroxamic acid (**X**) [31], hydroxy ethylnicotinic acid ester (**XI**) [32] and amino acids (**XII**) [33] (Fig. 2).

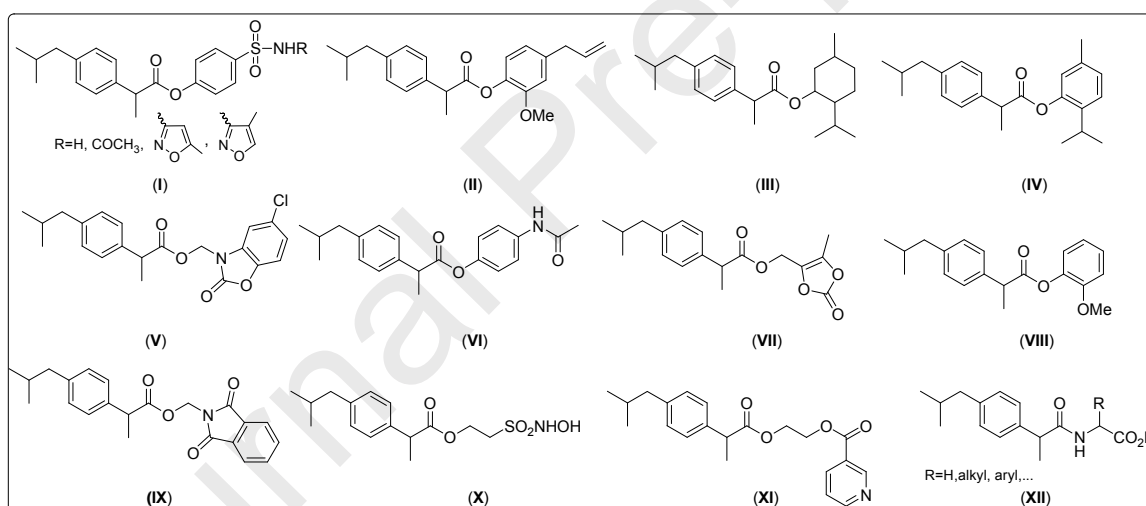


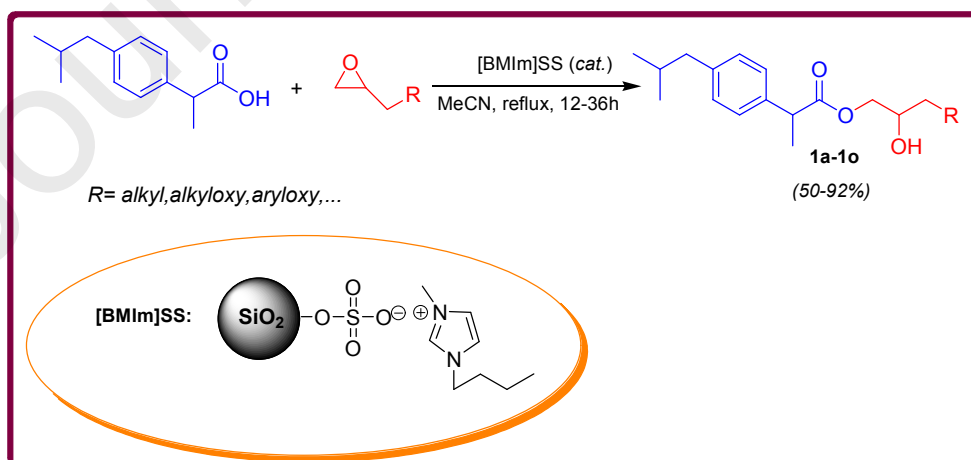
Fig. 2. Structure of some conjugated drugs and molecules with IBP.

Additionally, IBP was converted to related amides [34, 35] and esters [36] through the reaction with simple or functionalized amines and alcohols. It is also worthy to mention that IBP has been covalently tethered to diverse polymers in order to carry the drug and slow release of IBP in controlled release systems [37-39].

In recent decades, the heterogeneous catalysts have received increasing applications in organic transformations owing to their environmentally benign nature and plenty of remarkable advantages such as the ease of handling and separation, inexpensiveness, high selectivity, chemical and thermal

constancies [40]. Among the heterogeneous catalysts, the organic-inorganic hybrid catalysts (OIHCs) have found particular attention [41]. Silica-based OIHCs are fascinating since silica is plentifully available and displays high durability [42]. Silica sulfuric acid (SSA) is an environmentally benign silica-based heterogeneous catalyst that has been used in many organic reactions [43]. Additionally, the butyl methyl imidazolium (BMIm) salts have been extensively applied in many organic transformations either as ionic liquids or catalysts [44]. In current decades, there has been an enormous interest in immobilization of ILS on various inorganic and polymeric supports. The supported ILS or SILs are significant owing to their ILS concomitant, high catalytic activity, ease of separation and recoverability which largely increase their applicability in industrially important catalytic processes [45-47].

As explained earlier, the application of IBP in its parental shape often provides several side effects and disorders in patients. To reduce the side effects, the strategy of conversion of IBP into related prodrugs is traditionally applied. One way for preparation of IBP prodrug is conversion of IBP to related 1,2-diol monoester which through the best of our knowledge has not yet reported so far. Additionally, since the remarkable advantageous of OIHCs as a heterogeneous nano catalyst, hereby we would like to report the synthesis and characterization of butyl methyl imidazolium silica sulfate [BMIm]SS as a novel nano hybrid catalyst and its application in synthesis of new IBP 1,2-diol monoesters (**1a-1o**) as potent analgesic and anti-inflammatory agents (Scheme 1).

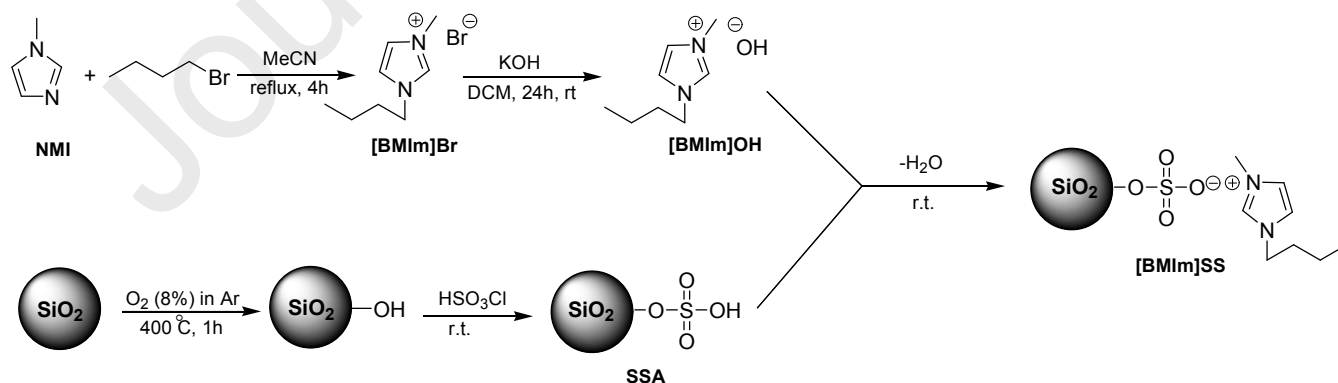


Scheme 1. Synthesis of new IBP 1,2-diol monoester catalyzed by [BMIm]SS.

2. Results and Discussion

2.1. Preparation of [BMIm]SS

The process for the preparation of [BMIm]SS is shown in Scheme 2. Due to Scheme 2, primarily, the butyl methyl imidazolium bromide [BMIm]Br was prepared via the reaction of N-methyl imidazole and butyl bromide in anhydrous acetonitrile as a solvent at reflux condition. Afterward of synthesis and purification of [BMIm]Br, it was diluted in anhydrous DCM in the presence of solid KOH at room temperature which was vigorously stirred to afford butyl methyl imidazolium hydroxide [BMIm]OH as a brown oil [48]. In another separate process, the traditional SiO₂ was first activated by a flow of 8% O₂ in an argon atmosphere at 400 °C in a furnace for an hour to acquire activated SiO₂. The use of O₂ flow at high temperature, produces the extra hydroxyl moieties at the surface of silica structure which is critically essential for tethering the active species. Afterward, the chlorosulfonic acid was added to activated-SiO₂ at ambient temperature to obtain the fresh silica sulfuric acid (SSA) due to literature [43]. Finally in an acid-base reaction, the SSA powder was suspended in deionized water and titrated with [BMIm]OH to reach a neutral pH (for control the pH, the pH-meter was used through the course of reaction). The reaction content was filtered to obtain a brown solid that washed several times with ethanol, dried *in vacuo* and stored in a vacuum desiccator at room temperature. The changes in color from SiO₂ to desired catalyst are shown in Fig. 3.



Scheme 2. Procedure for preparation of butyl methyl imidazolium silica sulfate [BMIm]SS as a catalyst.

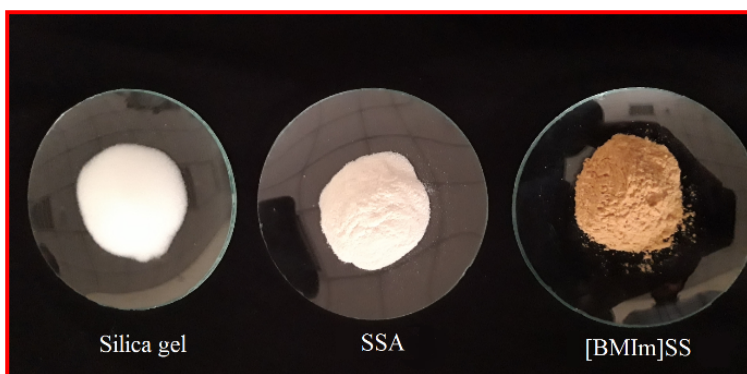


Fig. 3. The changes in color from silica gel to [BMIm]SS.

2.2. Characterization of catalyst

The powder X-ray diffraction pattern of the [BMIm]SS was obtained by the precipitation from freshly prepared aqueous [BMIm]SS suspension at 10–90 °C (Fig. 4). Based on the XRD pattern, the sample was an amorphous solid without regular crystalline lattice.

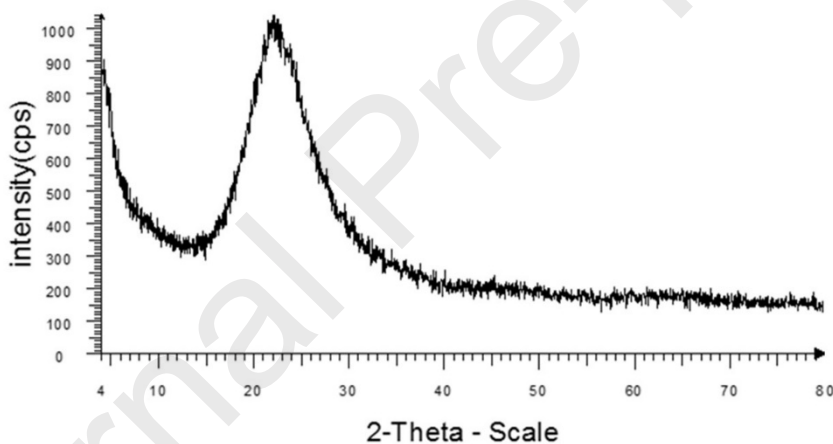


Fig. 4. XRD Pattern of the [BMIm]SS.

The scanning electron microscopy (SEM) image was applied to evaluate the size and morphology of the [BMIm]SS (Fig. 5). As can be seen in SEM images, the catalyst powders were produced in nano scales, and these particles were nearly spherical in morphology. Regarding to SEM analysis, using the microstructural image processing software (MIP software), the acquired histogram determined the particle size distribution around 20–25 nm (Fig. 6). The chemical composition of nanoparticles was also determined using Energy-dispersive X-ray spectroscopy (EDS) (Fig. 7). The EDS analysis has indicated the presence of elements like C, Si, N, O and S which is a good evidence for synthesis of [BMIm]SS.

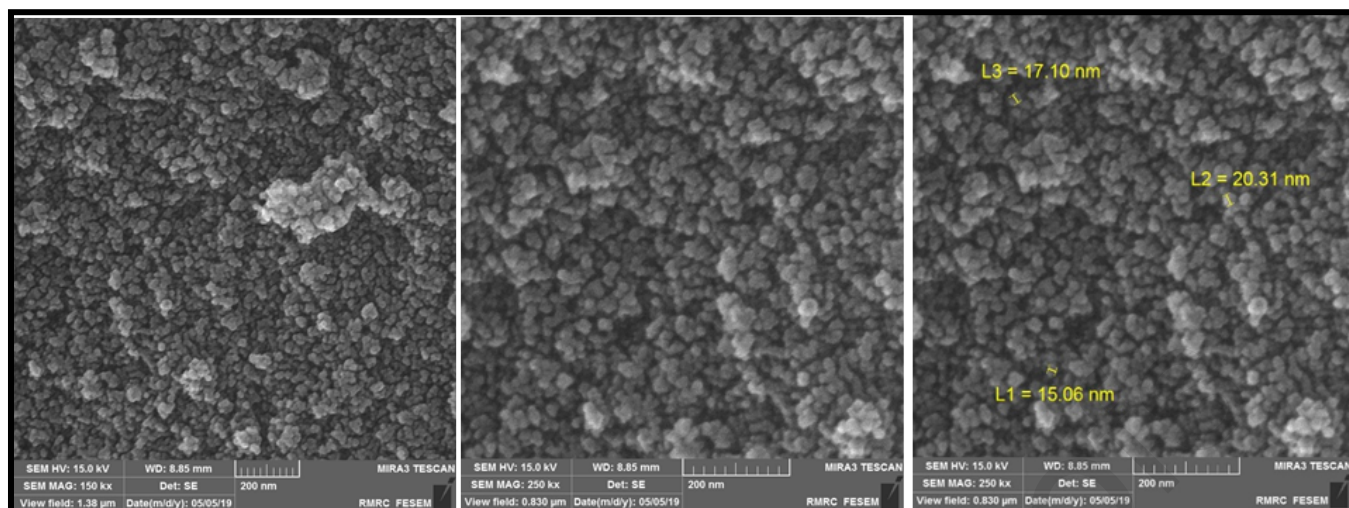


Fig. 5. Scanning electron microscopy (SEM) image of [BMIm]SS.

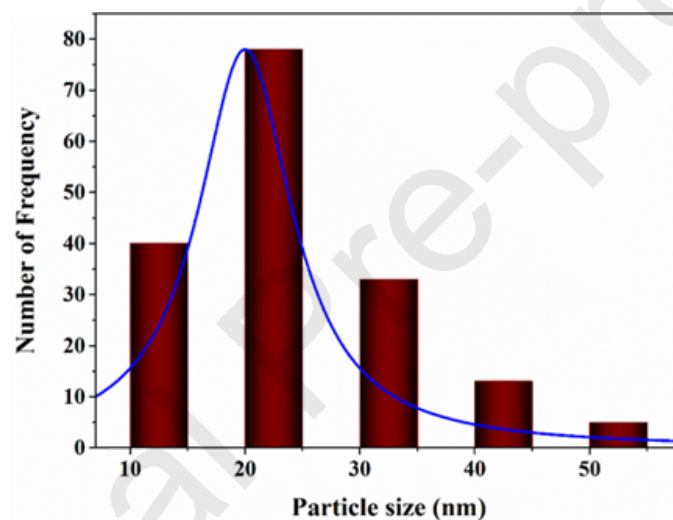


Fig. 6. Histogram representing the average diameter of [BMIm]SS.

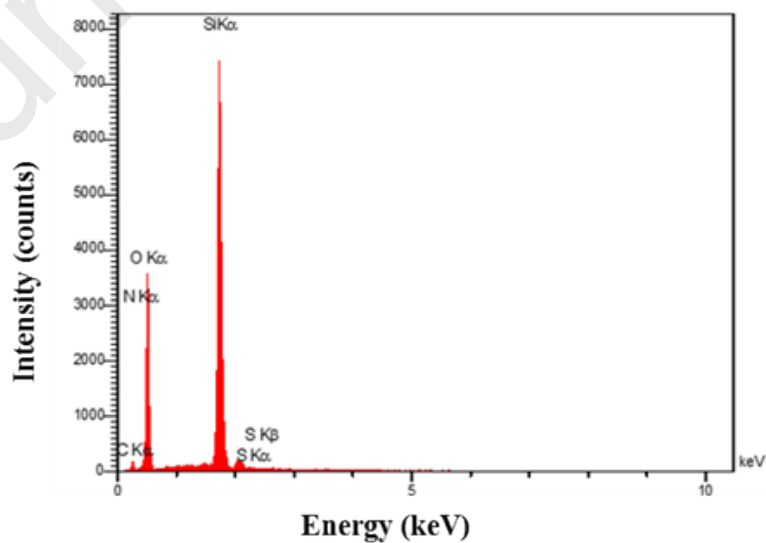


Fig.7. EDS Spectrum of [BMIm]SS.

The FT-IR spectrum of the [BMIm]SS is shown in Fig. 8. Since [BMIm]SS is a solid, the IR spectrum was recorded by the KBr disk technique. FT-IR spectra of silica gel, SSA and [BMIm]SS are shown and compared as spectra (A), (B) and (C), respectively (Fig. 8). In spectrum (A), the broad bending at 3600 cm^{-1} is related to the stretching frequency of the OH group on the silica gel substrate, and the broad bending at $1007\text{-}1200\text{ cm}^{-1}$ is related to the symmetric and anti-symmetric stretching frequency of the Si-O-Si bond which also are observed for both SSA and [BMIm]SS. A peak pertaining to S=O at 1200 cm^{-1} which overlaps with Si-O-Si peak is a good criterion for grafting of sulphonic acid on silica gel surface (B, C). Finally, in spectrum (C), an absorption band at $2850\text{-}2950\text{ cm}^{-1}$ is assigned to CH which is a good evidence for loading the organic residue into the inorganic part.

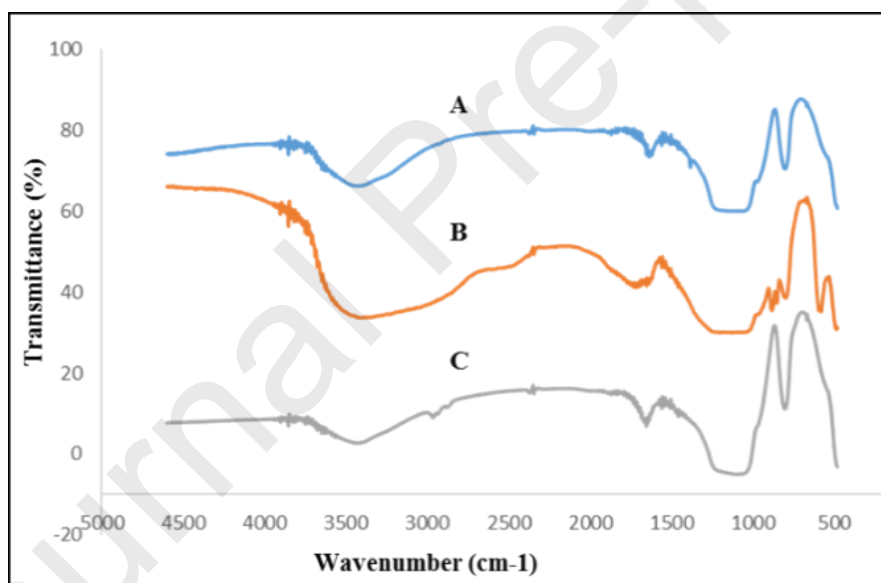


Fig. 8. FT-IR Spectrum of the silica gel (A), SSA (B) and [BMIm]SS (C).

The thermogravimetric (TGA) analysis for [BMIm]SS performed at weight of sample in heating rate of $10\text{ }^{\circ}\text{C min}^{-1}$ in N_2 atmosphere within temperature range $26\text{-}900\text{ }^{\circ}\text{C}$. The thermogram of [BMIm]SS is shown in Fig. 9. The thermogram of the catalyst indicated a thermal stability of [BMIm]SS around 200°C with mass loss ($\approx 2\%$) below $100\text{ }^{\circ}\text{C}$, due to removal of physically adsorbed water from the sample. As shown by TGA analysis, the thermal degradation of [BMIm]SS began at temperatures above $200\text{ }^{\circ}\text{C}$, which was attributed to the loss of organic residue loaded onto the silica surface and continues to $400\text{ }^{\circ}\text{C}$.

Subsequent weight loss that occurred at temperatures above 600 °C was related to the inorganic part of the catalyst. In general, the [BMIm]SS nearly lost 15% of its overall weight at 900 °C which is a good criterion for grafting of organic residue on the surface of silica.

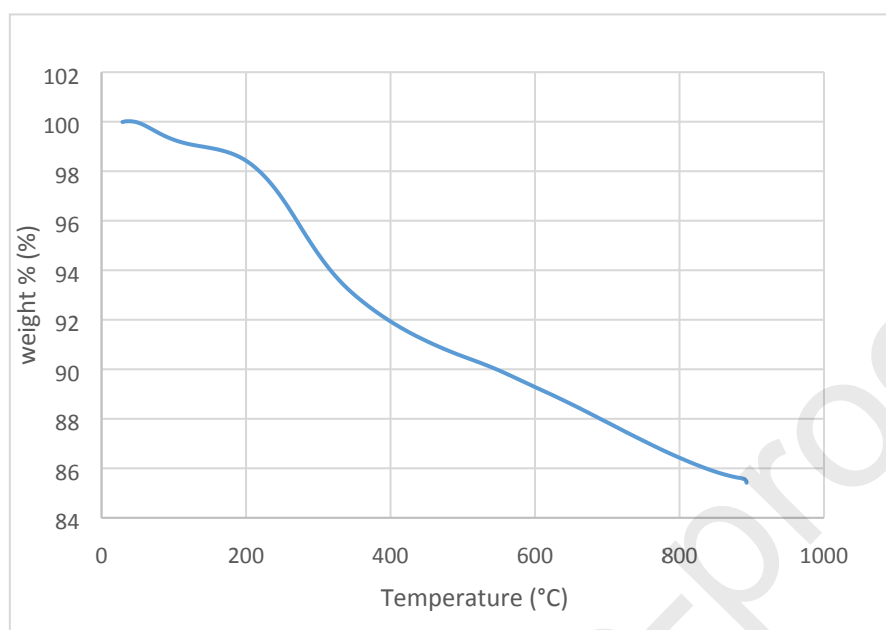


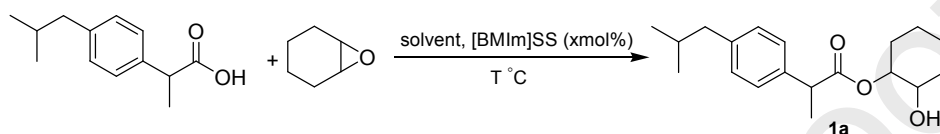
Fig.9. Thermogram of [BMIm]SS.

2.3. Synthesis of new 1,2-diol monoesters of IBP derivatives

The synthetic route to access the title compounds was performed due to general pathway illustrated in Scheme 1. In order to optimize the reaction conditions, we initially selected the ring opening of cyclohexene oxide with IBP as a model reaction. Firstly, it was attempted to optimize the factors influences in progress of reaction comprising solvent type, catalyst amount and temperature (Table 1). As shown in Table 1, the influence of diverse traditional solvents on sample reaction was explored (Table 1, entries 1-10) and it was indicated that among solvents acetonitrile provided the best result. Additionally, the use of acetone acquired a reasonable yield for **1a**; however, the other solvents were not appropriate enough to be considered as a reaction media. Next, to determine the optimized amount of [BMIm]SS, the different amounts of catalyst were applied on sample reaction (Table 1, entries 3 and 11-16). Prior to use of the catalyst, it was indicated by a simple titration that each 0.5 g of catalyst contains 1.22×10^{-3} mol% of [BMIm] species. Thus, the different amounts of [BMIm]SS were loaded to find out the

extent of reaction progress. As can be seen in Table 1, without the catalyst, the reaction was not conducted at all. In addition, the best result was obtained when 4.88×10^{-4} mol% (0.2 g) catalyst was employed. The use of larger amounts of catalyst did not have a tangible effect on progress of reaction. The effect of temperature was also assessed and revealed that the reaction was poorly achieved at ambient temperature and the maximum yield was obtained when the reaction was set to reflux condition.

Table 1. The influence of solvent type, catalyst amount and temperature on sample reaction. ^a



Entry	Solvent	[BMIm]SS (mol %)	T °C	Time (h)	Yield (%) ^b
1	DMF	4.88×10^{-4}	100	36	46
2	DMSO	4.88×10^{-4}	100	48	32
3	MeCN	4.88×10^{-4}	reflux	24	90
4	HMPT	4.88×10^{-4}	100	48	36
5	NMP	4.88×10^{-4}	100	36	41
6	THF	4.88×10^{-4}	reflux	48	51
7	Toluene	4.88×10^{-4}	reflux	48	57
8	Acetone	4.88×10^{-4}	reflux	24	69
9	PEG 200	4.88×10^{-4}	100	48	38
10	H ₂ O	4.88×10^{-4}	reflux	72	NR ^c
11	MeCN	0	reflux	72	NR
12	MeCN	1.22×10^{-4}	reflux	24	33
13	MeCN	2.44×10^{-4}	reflux	24	50
14	MeCN	3.66×10^{-4}	reflux	24	67
15	MeCN	6.10×10^{-4}	reflux	24	90
16	MeCN	7.32×10^{-4}	reflux	24	90
17	MeCN	4.88×10^{-4}	15	36	22
18	MeCN	4.88×10^{-4}	20	36	24
19	MeCN	4.88×10^{-4}	50	36	63
20	MeCN	4.88×10^{-4}	75	24	72

^a Reaction conditions: IBP (10 mmol), cyclohexene oxide (12 mmol), [BMIm]SS (xmol %) and solvent (30 mL).

^b Isolated yield.

^c No reaction.

With the optimal reaction conditions in hand, we screened the versatility and the scope of this protocol using [BMIm]SS as a catalyst. In this regard, the optimized reaction conditions were extended to the reaction of a variety of structurally diverse epoxides with IBP. Good to excellent yields of the

corresponding IBP 1,2-diol monoesters were obtained through the reaction of IBP with cyclohexene oxide and some terminal epoxides bearing diverse functionalities. Also, good regioselectivity was observed for the reaction of IBP with terminal epoxides using [BMIm]SS as a catalyst. In this regard, the ring opening of terminal epoxides was chiefly happened from their less hindered sides (>90%) as indicated by GC analysis. The structure of synthesized compounds **1a-1o** is shown in Fig.10.

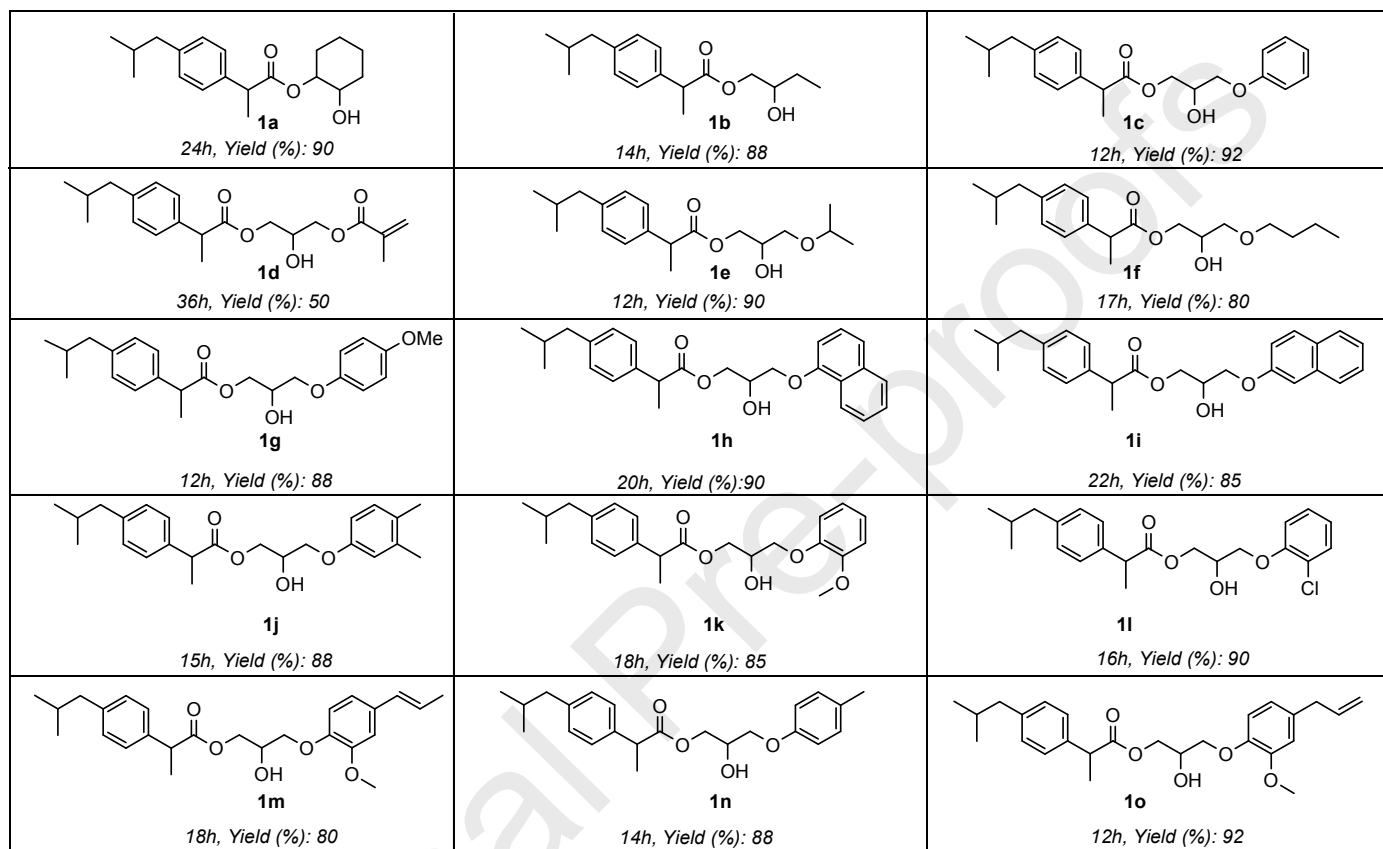
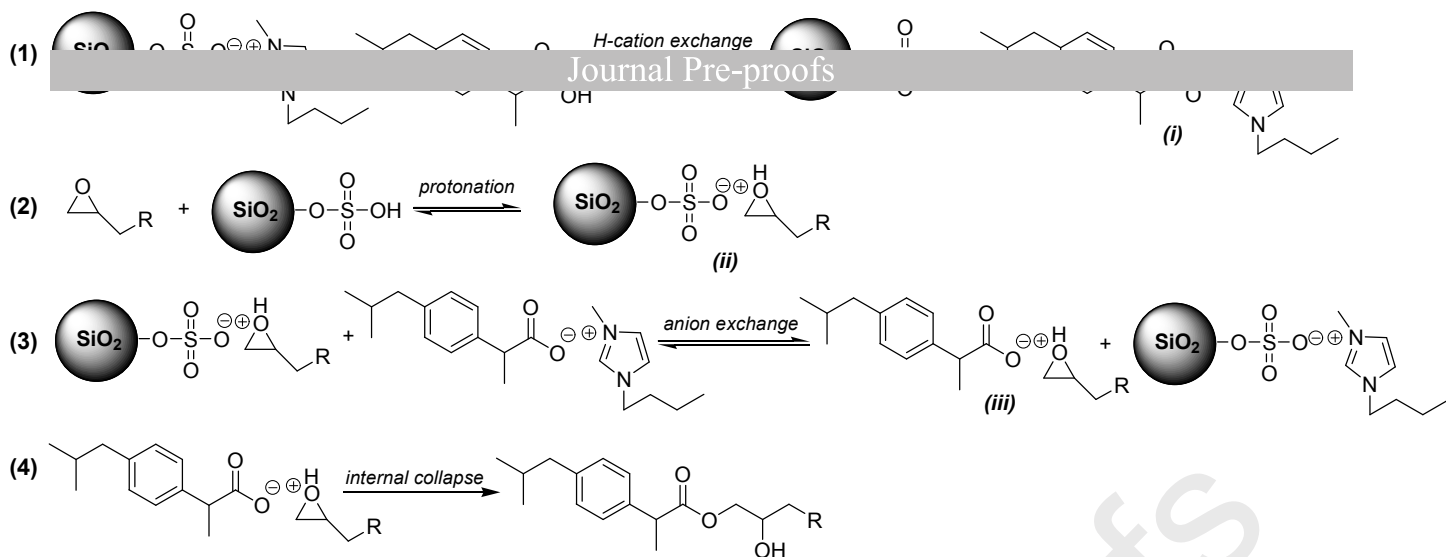


Fig. 10. Structure of novel 1,2-diol monoester of IBP.

As shown before, without the catalyst, the reaction was not conducted at all even in trace amount, hence the catalyst has undeniable role in progress of reaction. As it is well indicated, for the ring opening of epoxides, the presence of nucleophilic, basic or acidic conditions are usually essential. However neither MeCN nor IBP are known as strong nucleophile and acid, respectively. For example, IBP is a weak acid with $pK_a=5.3$ [49] which does not seem to be able to catalyze the reaction alone. Previously, we reported that the [BMIm]Br as an efficient base-free media for ring opening of epoxide via carboxylic acids [50]. In the same circumstances, we proposed a plausible mechanism for the ring opening of epoxides via IBP that catalyzed by [BMIm]SS (Scheme 3).

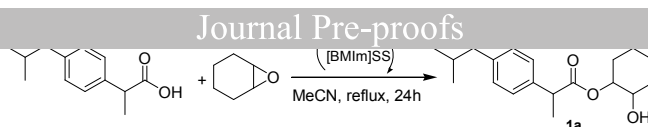


Scheme 3. A plausible mechanism for [BMIm]SS catalyzed the reaction of IBP and epoxides.

As can be seen in Scheme 3, in an initial step, because of ionic nature of immobilized ionic liquid on surface of [BMIm]SS, the strong electrostatic interaction between IBP and [BMIm]SS causes the dissociation of IBP followed by hydrogen-cation exchange which acquires SSA and [BMIm]ibuprofenate (**i**). Next (Step 2), the *in situ* generated SSA transfers the proton to epoxide to provide SSA-epoxide conjugate (**ii**). Then, through an anion exchange between (**i**) and (**ii**), an adduct of ibuprofenate-epoxide (**iii**) is generated followed by regeneration of [BMIm]SS (Step 3). Finally, the irreversible internal collapse of (**iii**) results in 1,2-diol mono-esters of IBP.

2.4. The reusability of [BMIm]SS

To assess the reusability of [BMIm]SS, this catalyst was applied for synthesis of **1a** as a sample reaction after several consecutive runs. To this end, after each run, the reaction mixture was filtered *in vacuo* through a sintered-glass funnel, and the residual solid was washed consecutively with ethanol and dried in a vacuum oven at 90 °C for 1h. The catalyst was then reused promptly without further purification, and no fresh catalyst was charged in latter runs. The catalyst was examined in seven consecutive runs which the results are depicted in Table 2. Due to obtained results (Table 2), the [BMIm]SS can be recycled and reused for successive trials without remarkable loss of its activity.

Table 2. The reusability of [BMIm]SS in successive trails for synthesis of **1a**.^a

Run	Time (h)	Yield (%) ^b
1	24	90 ^c
2	24	90
3	24	89
4	24	87
5	24	84
6	24	81
7	24	79

^a Reagent and conditions: IBP (10 mmol), cyclohexene oxide (12 mmol), [BMIm]SS (4.88×10^{-4} mol%), MeCN (30 mL), 24 h

^b Isolated Yield

^c Fresh catalyst

2.5. Biological assessment

2.5.1. Formalin test

Formalin test is one of the standard tests for measuring pain response. In this study, animals' response to pain caused by formalin was measured [51].

Experiments were performed on female mice (25–30g, n=54) purchased and kept in Comparative and Experimental Medicine Center of Shiraz University of Medical Sciences, Shiraz, Iran. Animal selection, care and sacrifice protocols were adhered to the Animal Care Committee of Iran Veterinary Organization guidelines. The mice were kept under a standard 12 h light/dark cycle at 21 ± 2 °C with *ad libitum* access to food and water. Animals were randomly divided into 3 equal groups of control, positive control and treatment. Before the inception of the experiment, mice were moved to a testing lab for at least 60 min and put in the formalin testing boxes for habituation for at least 30 min. A mirror was placed underneath at a 45° angle to allow a clear view of the paws. The synthesized compounds **1a-1o** or IBP were dissolved in olive oil and were fed orally to mice 10 min before pain tests. The dose of 1 μ L per gram of mouse was prepared for synthesized compounds and each animal was then gavaged using a special needle. Formalin (1%, 20 μ L; SC) was subcutaneously injected into right hind foot. These behaviors were scored and recording in several times (5, 10, 15, 20, 25, and 30 min) after formalin injection. The total time taken (in seconds) to hold, lick, and bite the foot to which formalin was injected was measured at intervals of the

first 5 min for acute pain and up to 30 min as chronic pain. Any **1a-1o** that can reduce this time has a better analgesic effect. The selection of these time intervals as an indicator of acute and chronic pain was based on previous studies [52]. These studies have shown that the first 5 min after formalin injection, when the animal shows severe painful behaviors, indicates acute pain, and then the second phase, pain (chronic pain) begins that does not show severe painful behaviors. Motor response to pain was recorded in the form of numbers zero, 1, 2 and 3 due to Dubuisson and Dennis method [53, 54]. The zero number indicates the status that animal was in perfect balance while walking and its weight was distributed on both legs. The number 1 indicates the status that animal could not bear the weight of the body on the foot that was injected with formalin or had difficulty in walking. The number 2 indicates that the animal was lifting the paw to which formalin was injected and had no contact with the floor of the chamber and the number 3 indicates the status that animal licked or shook the formalin-injected paw. Pain score during 60 min was calculated as 12 blocks of 5 min, the average pain score in each block was calculated according to the following equation:

$$\text{Pain Score} = \frac{T_0 + T_1 + T_2 + T_3}{20}$$

In this equation, T_0 , T_1 , T_2 and T_3 , indicate the number of 15 seconds that the animal exhibited zero, 1, 2, and 3 behaviors over a 5-minute period, respectively.

The analgesic effect curves of synthetic compound, IBP, control and blank group were plotted. The pain scores versus time for the most potent compounds were shown in Fig. 11. As can be seen in Fig. 11, the synthetic compounds **1h**, **1o**, **1k**, **1e**, **1l** and **1c** showed the best analgesic activity in comparison with IBP, blank and control. The majority of tested compounds demonstrated the good activity at early stage of oral administration at 5 min. Among tested compounds, **1h** showed very strong activity compare to IBP and others with pain score of 0.66 at 5 min. The second potent compound was **1o** which displayed slightly weaker pain score at 5 min but exhibited equal activities with **1h** at other time intervals. It is worthy to mention that, when compounds **1h**, **1o** and **1k** were applied, the animals merely felt pain at 5 min while at other times they didn't feel pain at all. The analgesic effect curves pertaining to **1e**, **1l** and **1c** also proved the remarkable analgesic activity compare to parental IBP. The pain scores for **1a**, **1b**, **1d**, **1f**,

1g, 1i, 1j, 1m, and 1n which are not shown here also demonstrated stronger or equal activities in comparison with IBP at different time intervals (see the Electronic Supplementary Information).

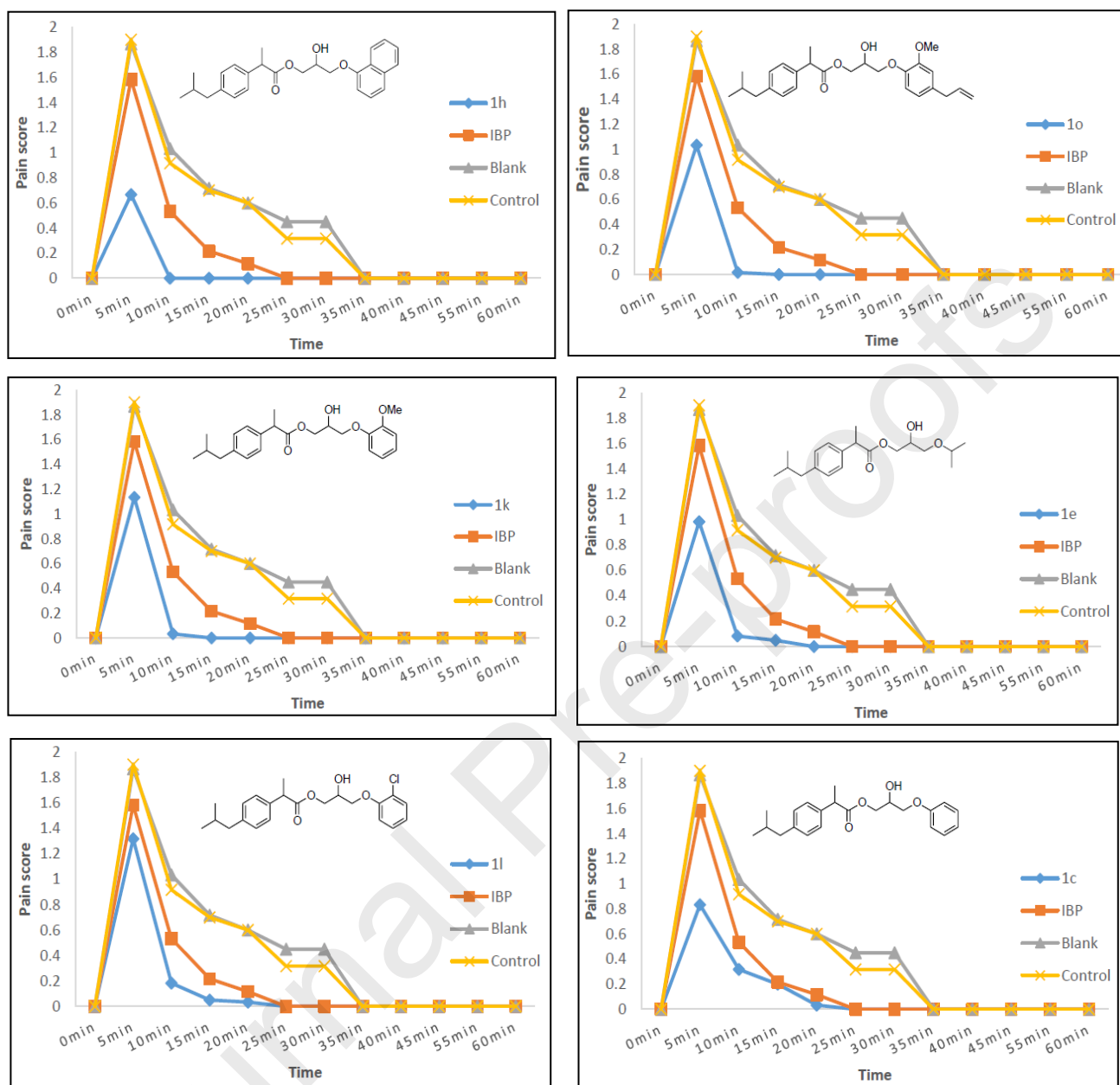


Fig.11. Analgesic effect curves of the most potent synthetic compounds **1h, 1o, 1k, 1e, 1l** and **1c**.

2.5.2. The acute pain and chronic pain

In Fig. 12, the comparison of the mean pain scores in the acute and chronic stages of the formalin test between compounds, IBP, blank, and control groups are given. Long-term pain is called chronic or persistent pain and the pain which is quickly relieved is called acute pain. For this purpose, we considered mice's pain for the first 5 min of acute pain and averaged pain for 30 min for chronic pain. As can be seen in Fig. 12, the most potent compounds **1h, 1o, 1k, 1e, 1l** and **1c** had better acute and chronic pain scores than IBP. Also **1f** and **1g** demonstrated lower acute and chronic pain scores than IBP, whereas **1d, 1i** and **1m** displayed poor performance from both acute and chronic pain aspects (see the

Electronic Supplementary Information). Furthermore, **1a** showed better performance for chronic pain but exhibited higher pain score for acute pain. However, **1b** displayed the opposite effect of **1a** against acute and chronic pains. In general, the animals felt less pain if the synthesized compounds were used either after 5 minutes or more. Thus, it can be concluded that IBP 1,2-diol monoesters not only could be used to treat the acute pain but also the chronic pain.

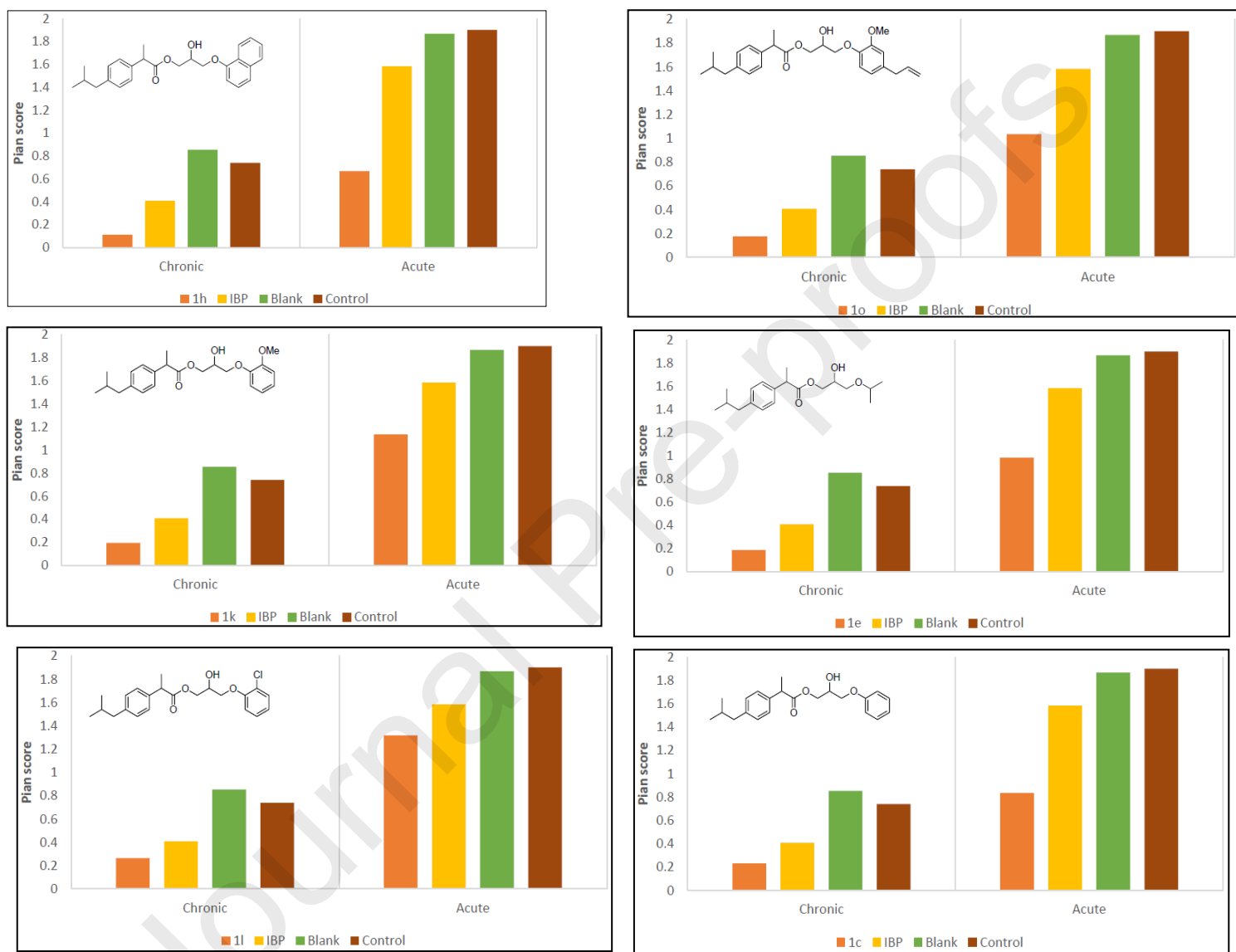


Fig. 12. The comparison of the mean pain scores in the acute and the chronic pain for the most potent compounds **1h**, **1o**, **1k**, **1e**, **1l** and **1c**.

2.5.3. Toxicity studies

The  Journal Pre-proofs was recorded. No mortality was observed due to the toxicity of the synthesized compounds.

2.6. Molecular docking study

Nowadays, molecular docking study is well-established as a powerful tool for prediction of probable interactions between drugs/drug candidates and target receptor/enzyme binding sites. Since some of our studied compounds exhibited good to excellent analgesic activity, we were encouraged to investigate their binding mode in the active site of target protein. In this context, the docking studies of compounds **1e**, **1h**, **1k**, and **1o** as the most potent compounds were assessed using Molegro Virtual Docker (MVD 6.0) software with its default settings [55]. Compounds **1i** and **1m** are the structural isomers of **1h** and **1o**, respectively which showed weak analgesic activity. The question that comes to mind, why the difference in position of naphthyl moieties (α in **1h** and β in **1i**) caused the remarkable difference in activity between **1h** and **1i**? In addition, why the change in position of a double bond from allyl in **1o** to vinyl in **1m** also resulted in activity gap? To answer these questions, the docking studies for **1i** and **1m** were achieved to gain a correlation between their activity and interaction with an active site of enzyme. Previously, it was reported that the anti-inflammatory and analgesic effects of IBP are due to the inhibition of COX-2 enzyme [56]. Therefore, the crystal structure of murine cyclooxygenase-2 (COX-2) in complex with IBP was selected as a template defined by PDB code: 4PH9. Initially, the ligand-bound crystallographic structure of COX-2 (4PH9) with 1.81 Å resolution was retrieved from the Protein Data Bank (<http://www.rcsb.org>). To modify the structure of selected enzyme, the assignment of hydrogen positions was achieved based on the default rules and all missing hydrogens were compensated. Then, the water molecules and the present ligands which are not involved in the binding of COX-2 enzyme and new ligand were removed. Afterward, the correct atom types and correct bond types were defined. The docking study was performed and reported based on 40 independent runs. The dock poses of selected compounds were analyzed to identify their interactions with COX-2 enzyme. Moreover, the definition of the active site of COX-2 enzyme was achieved by the amino acid residues within a 7Å radius around the ligands including IBP, **1e**, **1h**, **1i**, **1k**, **1m**, and **1o**. The geometry optimization of selected compounds and IBP was attained via DFT method at the B3LYP/6-311+G** level of theory using Gaussian09 program

package [57]. The validation of docking setup was performed through redocking of the co-crystallized IBP at the active site of COX-2. Previously, it was reported that RMSD value less than 2 Å is adequate to validate the docking setup [58]. The results indicated that the root-mean-square deviation (RMSD) value between the docked and co-crystallized IBP was 0.65 Å. Therefore, the validated docking protocol was applied to investigate the interaction and binding mode of compounds **1e**, **1h**, **1i**, **1k**, **1m**, and **1o** with the active site of COX-2 enzyme. An overlay view of docked conformations of **1e**, **1h**, **1i**, **1k**, **1m**, **1o** and IBP at the binding site of COX-2 enzyme is illustrated in Fig. 13. Interestingly, similar to IBP, **1e**, **1h**, **1i**, **1k**, **1m**, **1o** were located at the same binding site. However, due to their larger molecular size, a part of molecules were placed outside of the active site and interacts with amino acids near the active site.

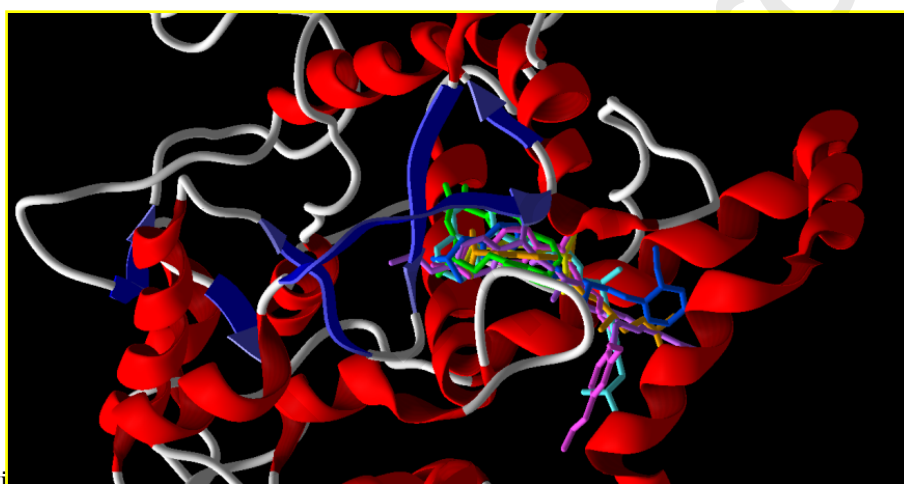


Fig. 13. Overlay view of docked conformations of **1e** (blue), **1h** (green), **1i** (cyan), **1k** (magenta), **1m** (violet), **1o** (pink) and IBP (yellow) in binding site of COX-2 enzyme.

IBP was located near the apex of COX-2 active site during its binding to COX-2 enzyme [59]. Among the different amino acids near the entrance of the active site of COX-2 enzyme, Arg121 and Tyr356 play an important role for desirable interaction of enzyme with IBP [60]. Apparently, guanidinium moiety of Arg121 and the hydroxyl group of Tyr356 provided double and single H-bonds with the carboxylate group of IBP, respectively. In addition, the hydrophobic interactions between lipophilic parts of IBP and amino acids presented in the substrate channel, stabilized this compound in the active site of enzyme. Thus, Val350, Leu353, Val524, and Ala528 interacted with the benzyl moiety of IBP. Val350 and Leu360 made the hydrophobic interactions with α -Me group of IBP. Also, several hydrophobic interactions were detected between the isobutyl moiety of IBP and Leu353, Leu385, Trp388, Phe519, Met523, Val524,

Gly527, Ala528, and Ser531. The docked conformation and H-bonds of IBP in the active site of COX-2 enzyme are shown in Fig. 14.

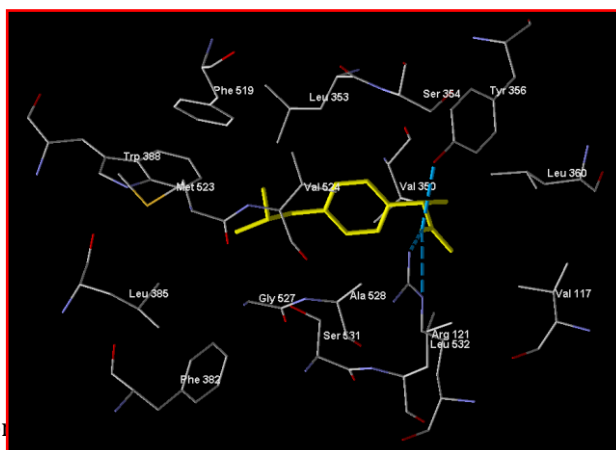
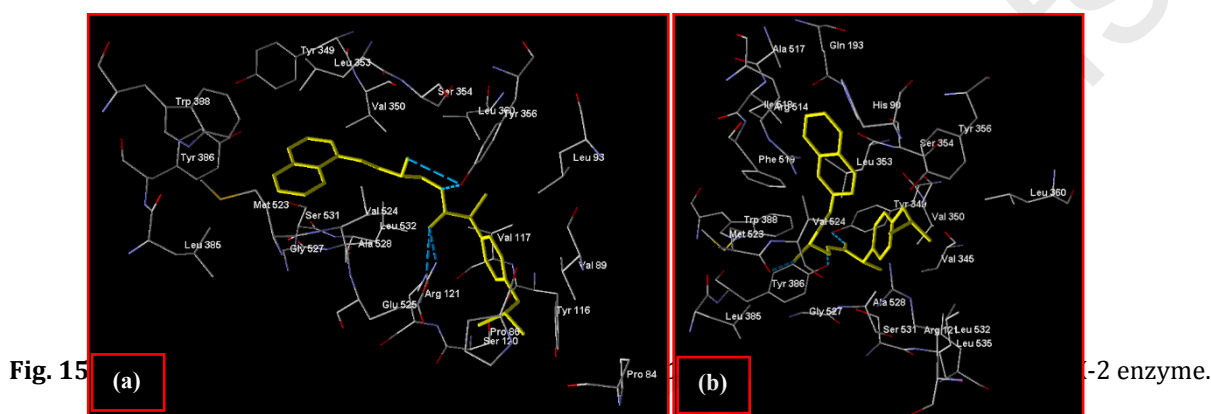


Fig. 14. Docked conformation and H-bonds of IBP in the active site of COX-2 enzyme.

Owing to apparent differences in activity of **1h** and **1i**, molecular docking study was achieved using MVD software to better understanding the correlation between the activity and the binding mode of compounds. Fig. 15 shows the docked conformation and H-bond of **1h** and **1i** in the active site of COX-2 enzyme. By default, MVD software identified five binding sites. As expected, **1h** was located in the active site where it also occupied by IBP. Due to the larger size of **1h** in comparison with IBP and small size of active site, a part of **1h** was located outside of the active site cavity and provided extra binding like hydrophobic interactions with other amino acids near the active site. The carboxylate group of **1h** participated in double H-bonds with Arg121 and single H-bond with Tyr356 which stabilized **1h** in the active site of enzyme (Fig. 15a). Also, the hydroxyl group of **1h** afforded additional H-bond with Tyr356. The α -naphthyl moiety of **1h** prepared the hydrophobic contacts with Tyr349, Val350, Leu353, Tyr386, Trp388, Met523, Val524, Gly527, Ala528, and Ser531. The rest of molecule involved some hydrophobic interactions with Pro86, Leu93, Val89, Tyr116, Val117, and Ser120 which are near the active site of enzyme.

Compound **1i** was twisted to some extent in the active site of enzyme and in contrary to **1h**, β -naphthyl of **1i** located outside of the active site and stabilized through non-bonded interactions with His90, Tyr349, Leu353, Trp388, Arg514, Ala517, Ile518, Phe519, and Val524 (Fig. 15b). The carboxylate group of **1i** contributed in H-bonds with Tyr349 and Tyr386. In addition, one H-bond interaction was detected between hydroxyl moiety of **1i** and Met523. The rest of molecule was placed in a pocket and interacted with Val345, Tyr349, Val350, Val524, Gly527, Ala528, and Ser531. The calculated ΔG values for IBP, **1h**

and **1i** were -97.73 , -164.22 and -167.87 (kcal/mol), respectively. While ΔG value for **1i** was more negative than ΔG value for IBP and **1n**; however, the analgesic activity of **1i** was less than those of IBP and **1h**. It seems that the H-bonding interaction of a ligand with both Arg121 and Tyr356 is essential for its analgesic activity. This hypothesis obviously can be confirmed by obtained results from docking and experimental studies where the lack of these H-bond interactions regarding **1i** caused the weak analgesic activity.



The docked conformation and H-bonds of **1m** are shown in Fig. 16a. As shown in Fig. 16a, the eugenolyl moiety of **1m** was placed outside of an active site and contributed in hydrophobic interactions with Val89, Val117, and Tyr116. Also, the isobutyl group of IBP core in **1m** located outward of the active site and interacted with Leu385, Tyr386, and Met 523. Thus, the isobutyl group lost numerous hydrophobic interactions with amino acids present in the active site. The benzyl and α -Me groups of IBP core interacted with a hydrophobic pocket consists of Val350, Leu353, Ser354, Phe519, Met523, Val524, Gly527, Ala528. The carboxylate, hydroxyl, phenoxy, and methoxy groups of **1m** participated in four H-bond interactions with Tyr356. Additionally, the triple H-bond interactions of Arg121 with hydroxyl and phenoxy groups were detected.

The docking analysis of **1o** revealed the contribution of carboxylate group in H-bond interaction with Tyr356. Also, the hydroxyl residue of **1o** afforded additional H-bond interactions with Arg121 and Tyr356 (Fig.16b). Due to larger size of **1o** compare to IBP, the eugenolyl moiety of **1o** located outside of the active site and participated in hydrophobic interactions with Pro86, Val89, Leu93, Val117, Ser120, and Ser472. The IBP core of **1o** was completely located in an active site and interacted with a

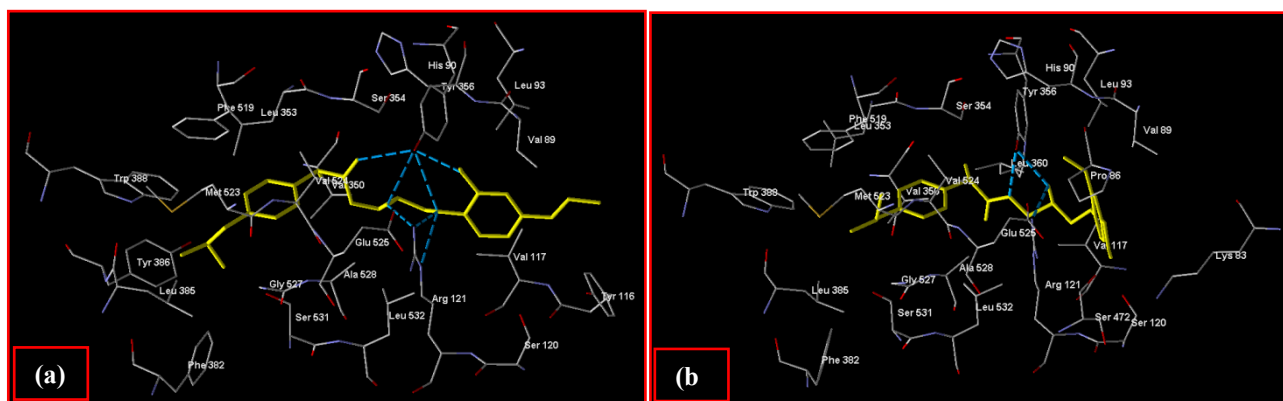


Fig. 16. Docked conformation and H-bonds (light blue) of **1m** (a) and **1o** (b) in active site of COX-2 enzyme.

The calculated ΔG values were -172.99 and -176.17 (kcal/mol) for **1m** and **1o**, respectively. Due to result, despite the energy gap for binding of **1m** and **1o** to the active site of COX-2 enzyme was negligible; however, their analgesic activities were not comparable. Obviously, the lack of proper hydrophobic interactions of the isobutyl group of IBP core in **1m** can be compensated by seven strong H-bond interactions to afford a ΔG value similar to that of **1o**. Considering the obtained results, it can be concluded that beside the H-bond interaction of a ligand with Arg121 and Tyr356 present in an active site of COX-2 enzyme, the proper hydrophobic interactions between a ligand and the active site of COX-2 enzyme played a vital role to determine the analgesic activity.

The docked conformation and H-bonds of compound **1e** are shown in Fig. 17a. The IBP core of **1e** was sited in the active site of COX-2 enzyme and interacted with a hydrophobic pocket formed by Val350, Leu353, Ser354, Leu360, Trp388, Phe519, Met523, Val524, Gly527, Ala528, Ser351, and Leu532. The carboxylate group afforded three H-bond interactions with Arg121 and one H-bond interaction with Tyr356. The hydroxyl group of **1e** participated in two H-bond interactions with Arg121 and Tyr356. The aliphatic chain of molecule oriented outward of the active site and interacted with Val89, Leu93, Ile113, Val117, Tyr116, and Ser120. In the case of **1k**, the IBP core of **1k** was placed in the active site and interacted with Val350, Leu353, Ser354, Leu385, Tyr386, Trp388, Phe519, Met523, Val524, Gly527, Ala528, and Ser531 (Fig. 17b). The carboxylate and hydroxyl groups of **1k** participated in four H-bond interactions with Arg121 and Tyr356. The rest of molecule was placed out of the active site and provided

non-bonded hydrophobic interactions with Val89, Leu93, Ile113, Val117, Phe358, and Leu360. The calculated ΔG values for **1e** and **1k** were -135.30 and -145.52 (kcal/mol), respectively. indeed, the obtained results from the docking study have confirmed the superior analgesic activity of **1e** and **1k** in comparison with IBP which is in a good agreement with the obtained experimental results.

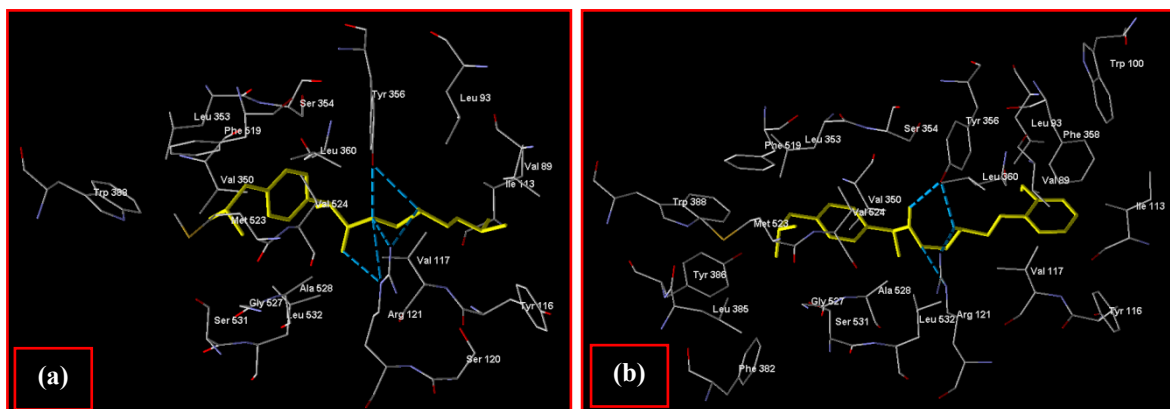


Fig. 17. Docked conformation and H-bonds (light blue) of **1e** (a) and **1k** (b) in active site of COX-2 enzyme.

2.7. Quantum study

The energy of the highest occupied molecular orbital (HOMO) and the lowest unoccupied molecular orbital (LUMO) were calculated at the B3LYP/6-31G** level of theory for the optimized structure of **1e**, **1h**, **1i**, **1k**, **1m**, **1o** and IBP to rationalize the binding affinity of these compounds (Table 3). The HOMO/LUMO views for the optimized geometry of the most potent compounds **1h**, **1o**, **1k** and IBP were shown in Fig. 18. The HOMO-LUMO energy gaps for **1e**, **1h**, **1i**, **1k**, **1m**, **1o** and IBP as well as the hardness and softness values were depicted in Table 3.

As depicted in Table 3, except that of **1e** which has a close softness with IBP, all other active compounds were softer than IBP and thus had more polarizability than IBP.

Table 3. Calculated HOMO, LUMO, hardness, and softness for **1e**, **1h**, **1i**, **1k**, **1m**, **1o** and IBP using B3LYP/6-31G** level of theory

Ligand	HOMO ^a	LUMO ^a	Softness ^a	Hardness ^b
1e	-6.670	-0.760	0.169	5.909
1h	-5.700	-1.134	0.219	4.567
1i	-5.733	-1.297	0.225	4.437
1k	-5.731	-0.798	0.203	4.933
1m	-5.427	-0.820	0.217	4.607
1o	-5.630	-0.794	0.207	4.836
IBP	-6.645	-0.766	0.170	5.879

^a Unit in electron volt (ev)

^b Unit in ev^{-1}

steric conditions for strong binding at active site of enzyme.

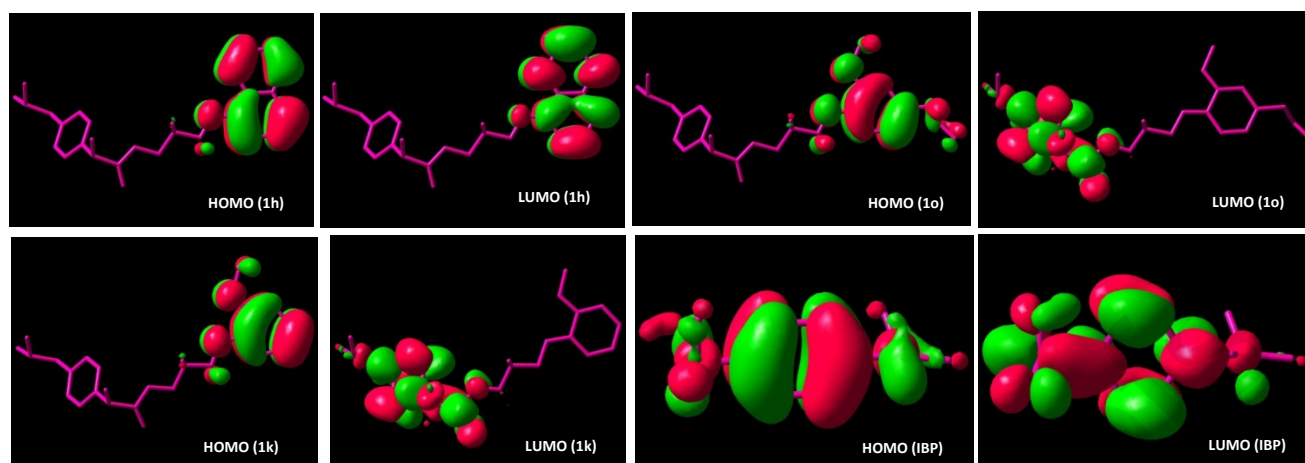


Fig. 18. HOMO and LUMO views for the optimized geometry of the most potent compounds **1h**, **1o**, **1k** and IBP.

2.8. *In silico* pharmacokinetic profile

Recently, the expanded approaches on the basis of *in silico* prognostication have found a powerful tool for methodical assessments of physiochemical properties [61]. In this regard, different physiochemical parameters and molecular descriptors were developed to estimate toxicity risks, drug likeness and drug scores in drug candidate molecules [62, 63]. The concept developed by Lipinski, so called Lipinski's rule of five (RO5), transpired as a simple way to predict the drug likelihood for candidate drugs. Due to RO5, a drug candidate should (i) have a molecular weight less than 500 Dalton, (ii) avoid more than 10 hydrogen bond acceptors (sum of N and O), (iii) exhibit 10 or fewer rotatable bonds, (iv) have an octanol-water partition coefficient (log P) value not more than 5; and (v) include the hydrogen bond donors (sum of NH and OH) less than 5. A drug candidate molecule that does not conform to these rules likely shows inferior pharmacokinetic profile for oral administration.

To study the *in silico* pharmacokinetic profile for synthesized compounds, we used a well-known and fully established OSIRIS DataWarrior V4.7.1 freeware [64]. This software encompasses the database for commercial none drug molecules or traded drugs. The risks of side effects, such as mutagenic, tumorigenic, irritant and reproductive effects, can be assessed using this software. The predicted toxicity risks by OSIRIS DataWarrior for all synthetic compounds and IBP were recorded in Table 4.

Table 4. Toxicity risks predicted by OSIRIS DataWarrior for all synthesized compounds and IBP.

Compound	Mutagenic	Tumorigenic	Reproductive Effective	Irritant
1a	None	None	None	None
1b	None	None	High	Low
1c	None	None	None	Low
1d	High	None	High	High
1e	None	None	None	None
1f	None	None	High	High
1g	None	None	None	None
1h	None	None	None	None
1i	None	None	None	None
1j	None	None	None	None
1k	None	None	None	None
1l	None	None	None	Low
1m	None	None	None	None
1n	None	None	None	High
1o	None	High	None	High
IBP	High	None	High	None

As indicated in Table 4, except that of **1d** and IBP as a reference drug, all synthesized compounds were predicted to exhibit none risk of mutagenic. Also except that of **1o**, other synthesized compounds and IBP were predicted to implicate none risk of tumorigenic. Furthermore, except that of **1b**, **1d**, **1f** and IBP that showed the reproductive effective, other studied compounds were anticipated to be harmless from reproductive effective point of view. In addition, IBP, **1a**, **1e**, **1g-1k** and **1m** were predicted to accommodate with no risk of irritant properties, whereas **1b**, **1c** and **1l** were predicted to involve the low risk. It is also worth mentioning that **1d**, **1f**, **1n** and **1o** were at high risk of irritant properties.

In addition to the toxicity risks prediction by OSIRIS DataWarrior, this software is capable to define some substantial descriptors or physiochemical parameters. To this end, we computed the Lipinski's parameters to show whether compounds are obeyed from Lipinski's R05 or not. As shown in Table 5, all computed molecular weights for compounds were ranged in 278.39–426.55 Dalton (<500 g/mol). Additionally, the number of hydrogen bond acceptors (nHba) for all compounds were 3–5 which conform the R05. The number of hydrogen bond donors (nHbd) for all compounds were equal to 1 which obeys from the Lipinski's R05. Apart from **1d**, **1f**, **1g**, **1k**, **1m** and **1o**, the other compounds involved the number of rotatable bonds (nrotb) between 6–10 which almost were similar to commercial drugs that lie within the range of R05 (Table 5).

One of the most important parameters in Lipinski's R05 is lipophilicity factor which traditionally is represented as an octanol–water partition coefficient (cLog P). Most known drugs were reported to have

the cLog P values <5. The cLog P values for all synthesized compounds were computed in range of 3.70–5.48. Except that of **1n**, **1i**, **1m** and **1o**, all others exhibited cLog P below to the defined limit by RO5 (<5).

The aqueous solubility of a molecule (cLog S) is an essential parameter that remarkably affects absorption and distribution specifications. Most common drugs have a cLog S value >−4. As can be seen in Table 5, except that of **1b**, **1d**, **1e** and **1f**, all compounds had the values less than indicated threshold value (<−4). Total polar surface area (TPSA) is an effective parameter for prediction of drug transport properties. TPSA is specified as a sum of surfaces of polar atoms (usually oxygen, nitrogen, and attached hydrogen) in a molecule. This parameter correlates very well with the human intestinal absorption and blood–brain barrier penetration. For most usual drugs, TPSA content are known to be less than 140 Å². As shown in Table 5, all synthesized compounds involved TPSA values less than 140 Å².

Table 5. Physicochemical properties predicted by OSIRIS DataWarrior software.

Compound	mw	nHba	nHbd	nrotb	cLogP	cLogS	TPSA	Drug likeness	Drug score
1a	304.43	3	1	6	4.14	-4.20	46.53	-3.69	0.35
1b	278.39	3	1	8	3.72	-3.46	46.53	-0.86	0.24
1c	356.46	4	1	10	4.29	-4.14	55.76	0.82	0.45
1d	348.44	5	1	11	3.70	-3.43	72.83	-23.48	0.08
1e	322.44	4	1	10	4.53	-3.49	55.76	0.82	0.66
1f	336.47	4	1	12	4.09	-3.65	55.76	-7.26	0.13
1g	386.49	5	1	11	4.22	-4.16	64.99	0.97	0.55
1h	406.52	4	1	10	5.48	-5.75	55.76	0.82	0.34
1i	406.52	4	1	10	5.48	-5.75	55.76	0.82	0.34
1j	384.51	4	1	10	4.98	-4.83	55.76	0.82	0.44
1k	386.49	5	1	11	4.22	-4.16	64.99	0.93	0.55
1l	390.91	4	1	10	4.90	-4.88	55.76	0.92	0.36
1m	426.55	5	1	12	5.31	-5.07	64.99	-1.20	0.28
1n	370.49	4	1	10	4.63	-4.49	55.76	0.82	0.30
1o	426.55	5	1	13	5.24	-4.87	64.99	-1.71	0.10
IBP	206.28	2	1	4	3.00	-2.90	37.30	0.08	0.24

Drug likeness is another parameter that predicted by current software. Among the compounds, **1a**, **1b**, **1d**, **1f**, **1m** and **1o** displayed negative drug likeness while the other compounds were found to have the positive values.

In addition, the software uses the above parameters to give the drug score to indicate whether it can be considered as a drug candidate or not. According to Table 5, **1e** and **1d** were indicated to have maximum and minimum drug score values, respectively. Regarding to all parameters like drug likeness, drug score and remarkable analgesic activity, **1h** can be suggested as an appropriate future drug candidate.

3. CONCLUSION

In summary, the fabrication, characterization and application of butyl methyl imidazolium silica sulfate [BMIm]SS as a novel nano hybrid catalyst and its application in synthesis of new IBP 1,2-diol mono esters were described. [BMIm]SS was proved to be an efficient nano-hybrid catalyst with thermal and chemical stability. This catalyst was a low cost and an environmentally benign that simply prepared and reused for many reaction runs without a significant decline in its reactivity. The synthesized compounds were tested *in vivo* for the analgesic properties on female mice using formalin test. The test results revealed that most compounds, especially **1c**, **1e**, **1h**, **1k**, **1l** and **1o** displayed potent analgesic activity compare to IBP as a reference drug. The docking analysis was conducted to gain a correlation between compound's activity and interaction with the active site of murine cyclooxygenase-2 (COX-2). The results confirmed stronger binding affinity of active compounds to active site of enzyme compare to IBP. The *in silico* pharmacokinetic profile, drug likeness and toxicity predictions were carried out for all compounds which determined **1h** as potent analgesic drug candidate for further investigations.

4. EXPERIMENTAL

4.1. General

All chemicals were purchased from Merck or Sigma-Aldrich. Solvents were purified by standard procedures, and stored over 3Å molecular sieves. Reactions were followed by TLC using SILG/UV 254 silica-gel plates. Column chromatography was performed on silica gel 60 (0.063–0.200 mm, 70–230 mesh; ASTM). IR spectra were obtained using a Shimadzu FT-IR-8300 spectrophotometer. GC/MS was performed on a Shimadzu GC/MS-QP1000-EX apparatus (m/z; rel. %). Elemental analyses were performed on a Perkin-Elmer 240-B micro-analyzer. ¹H- and ¹³C-NMR spectrum were recorded on Brüker Avance-DPX-250/400 spectrometer operating at 300/75 MHz, respectively. Chemical shifts are given in δ relative to tetramethylsilane (TMS) as an internal standard, coupling constants J are given in Hz. The scanning electron micrograph was achieved using SEM (VEGA//TESCAN-LMU) instrument. The patterned X-ray diffraction (XRD) was obtained using X'PERT PRO MPD Panalytical. The TGA test was performed using METTLER TOLEDO instrument. Data involving InChI (Key), ¹HNMR and ¹³CNMR for all products can be found in Electronic Supplementary Information.

4.2. General procedure for synthesis of [BMIm]SS

In a round-bottomed flask, butyl bromide (15 mmol) was added to the solution of N-methyl imidazole (10 mmol) in anhydrous acetonitrile (50 mL). The reaction mixture was then placed on magnetic stirrer for 4h under reflux condition to obtain butyl methyl imidazolium bromide [BMIm]Br. Afterward, to solution of [BMIm]Br (4 mmol) in 100 mL anhydrous DCM, it was added solid KOH (12 mmol) and stirred on magnetic stirrer for 24h at room temperature. Then, the reaction content was filtered by a sintered glass and the filtrate was evaporated to obtained almost pure [BMIm]OH as a brown oil [48]. Next, the SSA powder [43] was suspended in 100 mL deionized water and [BMIm]OH was added dropwise to the reaction vessel to finally reach a neutral pH (for control the pH, the pH-meter was used through the course of reaction). The obtained [BMIm]SS was filtered and washed several times with ethanol (3×10 mL). The [BMIm]SS was kept in a vacuum oven to dry completely and stored in a desiccator at room temperature.

4.3. General procedure for synthesis of new 1,2-diol monoester of IBP derivatives (**1a-1o**)

In a round-bottomed flask, it was added IBP (10 mmol), epoxide (12 mmol) and 0.2 g [BMIm]SS in 30 mL anhydrous acetonitrile. The reaction mixture was placed on magnetic stirrer under reflux conditions for 12-36h (Fig. 10). After completion of the reaction (TLC check), the catalyst was separated by a sintered glass, and the solvent was evaporated *in vacuo* (rotary evaporator). Then, the residue was diluted in CHCl₃ (150 mL) and washed with H₂O (3 × 150 mL). Afterward, the product was purified by a short column chromatography eluted by solvents described below.

4.4. Data for synthesized compounds

4.4.1. 2-hydroxycyclohexyl 2-(4-isobutylphenyl)propanoate (**1a**)

This compound was obtained as a yellow oil using column chromatography on silica gel (EtOAc:*n*-hexane, 1:20); Yield: 2.73 g, 90%; *R*_f = 0.46 (EtOAc:*n*-hexane, 1:3); IR (liquid film) ν_{\max} cm⁻¹ = 3500 (O–H, Stretch.), 3100 (sp² C–H, Stretch.), 2967 (sp³ C–H, Stretch.), 1740 (C=O, Stretch.), 1481 (aromatic C=C, Stretch.), 1410 (sp³ C–H, Bend.), 1150 (C–O, Stretch.), 890 (sp² C–H, Bend.). ¹H NMR (300 MHz, CDCl₃) δ_{ppm} = 0.90 (d, *J* = 6.6 Hz, 6H, (CH₃)₂CHCH₂), 1.06–1.35 (complex, 6H, 3CH₂), 1.47 (d, *J* = 7.2 Hz, 3H, CH₃CHCO₂), 1.57–1.67 (complex, 3H, CH₂, (CH₃)₂CHCH₂), 1.79–1.88 (complex, 2H, CHCO₂, CHOH), 2.42 (d, *J* = 7.2 Hz, 2H, PhCH₂), 2.71 (s, 1H, OH), 3.64–3.76 (m, 1H, CO₂CH), 7.06 (d, *J* = 8.1 Hz, 2H, aryl), 7.18 (d, *J* = 8.1 Hz, 2H,

aryl). ^{13}C NMR (75 MHz, CDCl_3) δ_{ppm} = 16.87 (C-12), 22.28 (C-20), 22.81 (C-21), 23.41 (C-9, C-10), 28.02 (C-22), 129.10 (C-2, C-4), 133.42 (C-6), 140.33 (C-3), 174.10 (C-13). MS (EI): m/z (%) = 304.20 (19.5) [M^+]. Anal. Calcd for $\text{C}_{19}\text{H}_{28}\text{O}_3$: C, 74.96; H, 9.27. Found: C, 75.09; H, 9.38.

4.4.2. 2-hydroxybutyl 2-(4-isobutylphenyl)propanoate (**1b**)

This compound was obtained as a yellow oil using column chromatography on silica gel (EtOAc:*n*-hexane, 1:20); Yield: 2.45 g, 88%; R_f = 0.66 (EtOAc:*n*-hexane, 1:3); IR (liquid film) ν_{max} cm^{-1} = 3500 (O–H, Stretch.), 3050 (sp^2 C–H, Stretch.), 2948 (sp^3 C–H, Stretch.), 1746 (C=O, Stretch.), 1438 (aromatic C=C, Stretch.), 1407 (sp^3 C–H, Bend.), 1167 (C–O, Stretch.), 860 (sp^2 C–H, Bend.). ^1H NMR (300 MHz, CDCl_3) δ_{ppm} = 0.90–0.92 (complex, 9H, CH_3CH_2 , $(\text{CH}_3)_2\text{CHCH}_2$), 1.42–1.63 (complex, 5H, CH_3CHCO_2 , CH_3CH_2), 1.79–1.92 (m, 1H, $(\text{CH}_3)_2\text{CHCH}_2$), 2.18 (s, 1H, OH), 2.45 (d, J = 7.2 Hz, 2H, PhCH_2), 3.66–3.79 (complex, 2H, CHOH , CHCO_2), 3.93–4.01 (m, 1H, OCH_AH_B), 4.11–4.18 (m, 1H, OCH_AH_B), 7.10 (d, J = 7.5 Hz, 2H, aryl), 7.20 (d, J = 7.8 Hz, 2H, aryl). ^{13}C NMR (75 MHz, CDCl_3) δ_{ppm} = 8.19 (C-20), 17.11 (C-12), 23.72 (C-9, C-10), 25.81 (C-18), 29.49 (C-8), 43.94 (C-11), 46.59 (C-7), 70.76 (C-16), 73.41 (C-17), 127.56 (C-1, C-5), 128.35 (C-2, C-4), 132.81 (C-6), 139.40 (C-3), 172.25 (C-13). MS (EI): m/z (%) = 278.19 (20.7) [M^+]. Anal. Calcd for $\text{C}_{17}\text{H}_{26}\text{O}_3$: C, 73.34; H, 9.41. Found: C, 73.23; H, 9.28.

4.4.3. 2-hydroxy-3-phenoxypropyl 2-(4-isobutylphenyl)propanoate (**1c**)

This compound was obtained as a yellow oil using column chromatography on silica gel (EtOAc:*n*-hexane, 1:20); Yield: 3.27 g, 92%; R_f = 0.60 (EtOAc:*n*-hexane, 1:3); IR (liquid film) ν_{max} cm^{-1} = 3400 (O–H, Stretch.), 3062 (sp^2 C–H, Stretch.), 2971 (sp^3 C–H, Stretch.), 1738 (C=O, Stretch.), 1463 (aromatic C=C, Stretch.), 1403 (sp^3 C–H, Bend.), 1280 (Ar–O, Stretch.), 1164 (C–O, Stretch.), 897 (sp^2 C–H, Bend.). ^1H NMR (300 MHz, CDCl_3) δ_{ppm} = 0.93 (d, J = 6.6 Hz, 6H, $(\text{CH}_3)_2\text{CHCH}_2$), 1.54 (d, J = 7.2 Hz, 3H, CH_3CHCO_2), 1.82–1.93 (m, 1H, $(\text{CH}_3)_2\text{CHCH}_2$), 2.49 (d, J = 7.2 Hz, 2H, PhCH_2), 3.12 (br s, 1H, OH), 3.76–3.91 (complex, 3H, CHCO_2CH_2), 4.17–4.37 (complex, 3H, CHOH , CH_2OPh), 6.87–7.33 (complex, 9H, aryl). ^{13}C NMR (75 MHz, CDCl_3) δ_{ppm} = 15.96 (C-12), 22.77 (C-9, C-10), 29.56 (C-8), 40.98 (C-11), 46.35 (C-7), 67.44 (C-16), 69.24 (C-17), 70.66 (C-18), 115.36 (C-22, C-26), 121.79 (C-24), 128.23 (C-1, C-5), 128.94 (C-2, C-4), 129.68 (C-23, C-25), 133.94 (C-6), 141.45 (C-3), 158.96 (C-21), 175.08 (C-13). MS (EI): m/z (%) = 356.20 (22.8) [M^+]. Anal. Calcd for $\text{C}_{22}\text{H}_{28}\text{O}_4$: C, 74.13; H, 7.92. Found: C, 74.01; H, 7.78.

4.4.4. 2-hydroxy-3-(2-(4-isobutylphenyl)propanoyloxy)propyl methacrylate (**1d**)

This compound was obtained as a yellow oil using column chromatography on silica gel (EtOAc:*n*-hexane, 1:10); Yield: 1.74 g, 50%; R_f = 0.49 (EtOAc:*n*-hexane, 1:3); IR (liquid film) ν_{max} cm^{-1} = 3500 (O–H, Stretch.), 3037 (sp^2 C–H, Stretch.), 2960 (sp^3 C–H, Stretch.), 1750 (C=O, Stretch.), 1702 (conjugated C=O, Stretch.), 1469 (aromatic C=C, Stretch.), 1402 (sp^3 C–H, Bend.), 1160 (C–O, Stretch.), 865 (sp^2 C–H, Bend.). ^1H NMR (300 MHz, CDCl_3) δ_{ppm} = 0.89 (br s, 6H, $(\text{CH}_3)_2\text{CHCH}_2$), 1.50 (br s, 3H, CH_3CHCO_2), 1.83–1.95 (complex, 3H,

(CH₃)₂CHCH₂), 2.44 (br s, 3H, CH₃C=CH₂), 3.64–4.18 (complex, 7H, OH, CHCO₂, OCH₂CHCH₂O), 5.60 (s, 1H, =CH_A), 19.13 (C-24), 23.78 (C-9, C-10), 30.65 (C-8), 41.12 (C-11), 46.15 (C-7), 68.52 (C-16), 69.24 (C-17), 70.32 (C-18), 125.86 (C-23), 128.10 (C-1, C-5), 129.47 (C-2, C-4), 132.70 (C-6), 137.03 (C-22), 140.29 (C-3), 168.07 (C-21), 174.19 (C-13). MS (EI): m/z (%) = 348.19 (18.6) [M⁺]. Anal. Calcd for C₂₀H₂₈O₅: C, 68.94; H, 8.10. Found: C, 69.09; H, 8.23.

4.4.5. 2-hydroxy-3-isopropoxypropyl 2-(4-isobutylphenyl)propanoate (**1e**)

This compound was obtained as a yellow oil using column chromatography on silica gel (EtOAc:*n*-hexane, 1:10); Yield: 2.90 g, 90%; *R*_f = 0.66 (EtOAc:*n*-hexane, 1:3); IR (liquid film) ν_{\max} cm⁻¹ = 3540 (O–H, Stretch.), 3041 (sp² C–H, Stretch.), 2952 (sp³ C–H, Stretch.), 1742 (C=O, Stretch.), 1449 (aromatic C=C, Stretch.), 1412 (sp³ C–H, Bend.), 1137 (C–O, Stretch.), 890 (sp² C–H, Bend.). ¹H NMR (300 MHz, CDCl₃) δ_{ppm} = 0.86 (d, *J* = 6.6 Hz, 6H, (CH₃)₂CHCH₂), 1.06 (d, *J* = 5.7 Hz, 6H, (CH₃)₂CHO), 1.44 (d, *J* = 6.9 Hz, 3H, CH₃CHCO₂) 1.77–1.85 (m, 1H, (CH₃)₂CHCH₂), 2.39 (d, *J* = 7.2 Hz, 2H, PhCH₂), 3.22–3.47 (complex, 4H, 2OCH₂), 3.67–3.73 (m, 1H, (CH₃)₂CHO), 3.84–3.89 (m, 1H, CHCO₂), 4.09 (br s, 2H, OH, CHOH), 7.04 (d, *J* = 7.8 Hz, 2H, aryl), 7.17 (d, *J* = 7.8 Hz, 2H, aryl). ¹³C NMR (75 MHz, CDCl₃) δ_{ppm} = 15.72 (C-12), 21.91 (C-9, C-10), 26.29 (C-22, C-23), 30.63 (C-8), 42.62 (C-11), 46.61 (C-7), 68.04 (C-16), 68.77 (C-17), 70.94 (C-18), 73.49 (C-21), 127.98 (C-1, C-5), 128.70 (C-2, C-4), 132.35 (C-6), 141.03 (C-3), 172.65 (C-13). MS (EI): m/z (%) = 322.21 (20.1) [M⁺]. Anal. Calcd for C₁₉H₃₀O₄: C, 70.77; H, 9.38. Found: C, 70.93; H, 9.56.

4.4.6. 3-butoxy-2-hydroxypropyl 2-(4-isobutylphenyl)propanoate (**1f**)

This compound was obtained as a yellow oil using column chromatography on silica gel (EtOAc:*n*-hexane, 1:10); Yield: 2.69 g, 80%; *R*_f = 0.66 (EtOAc:*n*-hexane, 1:3); IR (liquid film) ν_{\max} cm⁻¹ = 3460 (O–H, Stretch.), 3046 (sp² C–H, Stretch.), 2985 (sp³ C–H, Stretch.), 1742 (C=O, Stretch.), 1465 (aromatic C=C, Stretch.), 1409 (sp³ C–H, Bend.), 1148 (C–O, Stretch.), 873 (sp² C–H, Bend.). ¹H NMR (300 MHz, CDCl₃) δ_{ppm} = 0.90–0.94 (complex, 9H, (CH₃)₂CHCH₂, CH₃CH₂), 1.28–1.52 (complex, 7H, CH₃CHCO₂, CH₃CH₂CH₂), 1.81–1.90 (m, 1H, (CH₃)₂CHCH₂), 2.44 (d, *J* = 6.9 Hz, 2H, PhCH₂), 3.32–4.16 (complex, 9H, CHCO₂, OCH₂CHCH₂O, OCH₂CH₂, OH), 7.09 (d, *J* = 7.5 Hz, 2H, aryl), 7.20 (d, *J* = 7.2 Hz, 2H, aryl). ¹³C NMR (75 MHz, CDCl₃) δ_{ppm} = 15.81 (C-24), 17.27 (C-12), 20.49 (C-23), 23.39 (C-9, C-10), 28.77 (C-8), 34.19 (C-22), 41.38 (C-11), 46.44 (C-7), 66.61 (C-16), 67.65 (C-17), 71.15 (C-21), 74.16 (C-18), 127.09 (C-1, C-5), 128.17 (C-2, C-4), 131.41 (C-6), 139.34 (C-3), 171.76 (C-13). MS (EI): m/z (%) = 336.23 (23.7) [M⁺]. Anal. Calcd for C₂₀H₃₂O₄: C, 71.39; H, 9.59. Found: C, 71.54; H, 9.77.

4.4.7. 2-hydroxy-3-(4-methoxyphenoxy)propyl 2-(4-isobutylphenyl)propanoate (**1g**)

This compound was obtained as a yellow oil using column chromatography on silica gel (EtOAc:*n*-hexane, 1:10); Yield: 3.40 g, 88%; *R*_f = 0.46 (EtOAc:*n*-hexane, 1:3); IR (liquid film) ν_{\max} cm⁻¹ = 3470 (O–H, Stretch.), 3029 (sp² C–H, Stretch.), 2955 (sp³ C–H, Stretch.), 1750 (C=O, Stretch.), 1471 (aromatic C=C, Stretch.),

1420 (sp³ C–H, Bend.), 1237 (Ar–O, Stretch.), 1140 (C–O, Stretch.), 891 (sp² C–H, Bend.). ¹H NMR (300 MHz, Journal Pre-proofs 7 (m,

1H, (CH₃)₂CHCH₂), 2.44 (d, *J* = 6.9 Hz, 2H, PhCH₂), 2.90 (s, 1H, OH), 3.77 (s, 3H, OCH₃), 3.81–4.33 (complex, 6H, CHCO₂, OCH₂CHCH₂O), 6.77–6.84 (m, 4H, aryl), 7.08 (d, *J* = 7.8 Hz, 2H, aryl), 7.20 (d, *J* = 7.8 Hz, 2H, aryl). ¹³C NMR (75 MHz, CDCl₃) δ_{ppm} = 15.04 (C-12), 21.68 (C-9, C-10), 30.16 (C-8), 40.05 (C-11), 44.84 (C-7), 54.78 (C-27), 68.04 (C-16), 68.77 (C-17), 71.72 (C-18), 114.75 (C-23, C-25), 115.86 (C-22, C-26), 128.02 (C-1, C-5), 129.16 (C-2, C-4), 132.83 (C-6), 139.45 (C-3), 150.10 (C-21), 153.05 (C-24), 174.37 (C-13). MS (EI): *m/z* (%) = 386.21 (24.5) [M⁺]. Anal. Calcd for C₂₃H₃₀O₅: C, 71.48; H, 7.82. Found: C, 71.62; H, 7.98.

4.4.8. 2-hydroxy-3-(naphthalen-1-yloxy)propyl 2-(4-isobutylphenyl)propanoate (**1h**)

This compound was obtained as a yellow oil using column chromatography on silica gel (EtOAc:*n*-hexane, 1:10); Yield: 3.65 g, 90%; *R_f* = 0.54 (EtOAc:*n*-hexane, 1:3); IR (liquid film) ν_{max} cm⁻¹ = 3475 (O–H, Stretch.), 3050 (sp² C–H, Stretch.), 2969 (sp³ C–H, Stretch.), 1743 (C=O, Stretch.), 1486 (aromatic C=C, Stretch.), 1415 (sp³ C–H, Bend.), 1270 (Ar–O, Stretch.), 1163 (C–O, Stretch.), 897 (sp² C–H, Bend.). ¹H NMR (300 MHz, CDCl₃) δ_{ppm} = 0.98 (d, *J* = 6.6 Hz, 6H, (CH₃)₂CHCH₂), 1.59 (d, *J* = 6.9 Hz, 3H, CH₃CHCO₂), 1.88–1.97 (m, 1H, (CH₃)₂CHCH₂), 2.52–2.56 (m, 2H, PhCH₂), 3.46 (s, 1H, OH), 3.79–4.46 (complex, 6H, CHCO₂, OCH₂CHCH₂O), 6.70 (d, *J* = 7.2 Hz, 1H, aryl), 7.11–7.52 (m, 8H, aryl), 7.86 (d, *J* = 6.3 Hz, 1H, aryl), 8.34 (d, *J* = 7.2 Hz, 1H, aryl). ¹³C NMR (75 MHz, CDCl₃) δ_{ppm} = 17.49 (C-12), 23.58 (C-9, C-10), 31.09 (C-8), 41.14 (C-11), 45.81 (C-7), 67.68 (C-16), 68.75 (C-17), 71.25 (C-18), 105.69 (C-26), 119.67 (C-24), 122.17 (C-27), 125.05 (C-28), 125.75 (C-25), 126.48 (C-29), 127.55 (C-22), 128.26 (C-30), 128.98 (C-1, C-5), 129.70 (C-2, C-4), 133.30 (C-6), 135.09 (C-23), 140.10 (C-3), 157.67 (C-21), 175.96 (C-13). MS (EI): *m/z* (%) = 406.21 (26.7) [M⁺]. Anal. Calcd for C₂₆H₃₀O₄: C, 76.82; H, 7.44. Found: C, 76.99; H, 7.58.

4.4.9. 2-hydroxy-3-(naphthalen-2-yloxy)propyl 2-(4-isobutylphenyl)propanoate (**1i**)

This compound was obtained as a yellow oil using column chromatography on silica gel (EtOAc:*n*-hexane, 1:10); Yield: 3.45 g, 85%; *R_f* = 0.46 (EtOAc:*n*-hexane, 1:3); IR (liquid film) ν_{max} cm⁻¹ = 3490 (O–H, Stretch.), 3083 (sp² C–H, Stretch.), 2950 (sp³ C–H, Stretch.), 1740 (C=O, Stretch.), 1472 (aromatic C=C, Stretch.), 1410 (sp³ C–H, Bend.), 1249 (Ar–O, Stretch.), 1150 (C–O, Stretch.), 881 (sp² C–H, Bend.). ¹H NMR (300 MHz, CDCl₃) δ_{ppm} = 0.94 (d, *J* = 6.6 Hz, 6H, (CH₃)₂CHCH₂), 1.60 (d, *J* = 6.9 Hz, 3H, CH₃CHCO₂), 1.84–1.94 (m, 1H, (CH₃)₂CHCH₂), 2.45 (br s, 2H, PhCH₂), 3.32 (s, 1H, OH), 3.84–4.37 (complex, 6H, CHCO₂, OCH₂CHCH₂O), 7.12–7.56 (complex, 7H, aryl), 7.77–7.85 (m, 4H, aryl). ¹³C NMR (75 MHz, CDCl₃) δ_{ppm} = 18.04 (C-12), 23.79 (C-9, C-10), 30.29 (C-8), 40.76 (C-11), 46.15 (C-7), 67.45 (C-16), 68.91 (C-17), 71.77 (C-18), 106.01 (C-22), 119.36 (C-26), 125.10 (C-29), 126.95 (C-28), 127.30 (C-27), 128.09 (C-30), 128.75 (C-1, C-5), 129.47 (C-2, C-4), 130.18 (C-24), 130.55 (C-25), 132.70 (C-6), 134.15 (C-23), 139.58 (C-3), 158.30 (C-21), 173.84 (C-13). MS (EI): *m/z* (%) = 406.21 (27.4) [M⁺]. Anal. Calcd for C₂₆H₃₀O₄: C, 76.82; H, 7.44. Found: C, 76.97; H, 7.60.

4.4.10. 3-(3,4-dimethylphenoxy)-2-hydroxypropyl 2-(4-isobutylphenyl)propanoate (**1j**)

This compound was obtained as a yellow oil using column chromatography on silica gel (EtOAc:*n*-hexane, 1:10); Yield: 3.38 g, 88%; $R_f = 0.60$ (EtOAc:*n*-hexane, 1:3); IR (liquid film) $\nu_{\max} \text{ cm}^{-1} = 3420$ (O–H, Stretch.), 3065 (sp^2 C–H, Stretch.), 2952 (sp^3 C–H, Stretch.), 1744 (C=O, Stretch.), 1461 (aromatic C=C, Stretch.), 1417 (sp^3 C–H, Bend.), 1245 (Ar–O, Stretch.), 1158 (C–O, Stretch.), 868 (sp^2 C–H, Bend.). $^1\text{H NMR}$ (300 MHz, CDCl_3) $\delta_{\text{ppm}} = 0.99$ (d, $J = 6.3$ Hz, 6H, $(\text{CH}_3)_2\text{CHCH}_2$), 1.59 (d, $J = 6.9$ Hz, 3H, CH_3CHCO_2), 1.91–1.97 (m, 1H, $(\text{CH}_3)_2\text{CHCH}_2$), 2.29 (s, 3H, CH_3Ph), 2.32 (s, 3H, CH_3Ph), 2.52 (d, $J = 6.6$ Hz, 2H, PhCH_2), 3.26 (s, 1H, OH), 3.83–4.35 (complex, 6H, CHCO_2 , $\text{OCH}_2\text{CHCH}_2\text{O}$), 6.66–7.32 (complex, 7H, aryl). $^{13}\text{C NMR}$ (75 MHz, CDCl_3) $\delta_{\text{ppm}} = 17.53$ (C-12), 18.26 (C-27), 19.32 (C-28), 22.91 (C-9, C-10), 30.14 (C-8), 40.52 (C-11), 46.27 (C-7), 68.17 (C-16), 69.24 (C-17), 71.39 (C-18), 112.35 (C-26), 114.11 (C-22), 127.06 (C-24), 128.12 (C-25), 128.84 (C-1, C-5), 129.56 (C-2, C-4), 133.15 (C-6), 138.20 (C-23), 140.35 (C-3), 155.79 (C-21), 175.17 (C-13). MS (EI): m/z (%) = 384.23 (24.9) [M^+]. Anal. Calcd for $\text{C}_{24}\text{H}_{32}\text{O}_4$: C, 74.97; H, 8.39. Found: C, 74.80; H, 8.23.

4.4.11. 2-hydroxy-3-(2-methoxyphenoxy)propyl 2-(4-isobutylphenyl)propanoate (**1k**)

This compound was obtained as a yellow oil using column chromatography on silica gel (EtOAc:*n*-hexane, 1:10); Yield: 3.28 g, 85%; $R_f = 0.40$ (EtOAc:*n*-hexane, 1:3); IR (liquid film) $\nu_{\max} \text{ cm}^{-1} = 3500$ (O–H, Stretch.), 3060 (sp^2 C–H, Stretch.), 2976 (sp^3 C–H, Stretch.), 1735 (C=O, Stretch.), 1429 (aromatic C=C, Stretch.), 1412 (sp^3 C–H, Bend.), 1277 (Ar–O, Stretch.), 1148 (C–O, Stretch.), 874 (sp^2 C–H, Bend.). $^1\text{H NMR}$ (300 MHz, CDCl_3) $\delta_{\text{ppm}} = 0.93$ (d, $J = 1.8$ Hz, 6H, $(\text{CH}_3)_2\text{CHCH}_2$), 1.53 (br s, 3H, CH_3CHCO_2), 1.87 (br s, 1H, $(\text{CH}_3)_2\text{CHCH}_2$), 2.47 (br s, 2H, PhCH_2), 3.78–4.29 (complex, 10H, CHCO_2 , $\text{OCH}_2\text{CHCH}_2\text{O}$, OH, OCH_3), 6.84–7.24 (complex, 8H, aryl). $^{13}\text{C NMR}$ (75 MHz, CDCl_3) $\delta_{\text{ppm}} = 17.22$ (C-12), 23.28 (C-9, C-10), 30.51 (C-8), 40.92 (C-11), 46.12 (C-7), 57.08 (C-27), 68.35 (C-16), 69.24 (C-17), 71.26 (C-18), 114.29 (C-23), 115.45 (C-26), 121.82 (C-24), 122.69 (C-25), 128.76 (C-1, C-5), 129.61 (C-2, C-4), 133.09 (C-6), 140.33 (C-3), 147.24 (C-21), 150.14 (C-22), 172.09 (C-13). MS (EI): m/z (%) = 386.21 (20.6) [M^+]. Anal. Calcd for $\text{C}_{23}\text{H}_{30}\text{O}_5$: C, 71.48; H, 7.82. Found: C, 71.67; H, 7.97.

4.4.12 3-(2-chlorophenoxy)-2-hydroxypropyl 2-(4-isobutylphenyl)propanoate (**1l**)

This compound was obtained as a yellow oil using column chromatography on silica gel (EtOAc:*n*-hexane, 1:10); Yield: 3.51 g, 90%; $R_f = 0.57$ (EtOAc:*n*-hexane, 1:3); IR (liquid film) $\nu_{\max} \text{ cm}^{-1} = 3510$ (O–H, Stretch.), 3093 (sp^2 C–H, Stretch.), 2940 (sp^3 C–H, Stretch.), 1732 (C=O, Stretch.), 1452 (aromatic C=C, Stretch.), 1421 (sp^3 C–H, Bend.), 1236 (Ar–O, Stretch.), 1145 (C–O, Stretch.), 1058 (Ar–Cl, Stretch.), 847 (sp^2 C–H, Bend.). $^1\text{H NMR}$ (300 MHz, CDCl_3) $\delta_{\text{ppm}} = 0.92$ (d, $J = 6.0$ Hz, 6H, $(\text{CH}_3)_2\text{CHCH}_2$), 1.52 (d, $J = 6.3$ Hz, 3H, CH_3CHCO_2), 1.84–1.88 (m, 1H, $(\text{CH}_3)_2\text{CHCH}_2$), 2.45 (d, $J = 6.3$ Hz, 2H, PhCH_2), 3.24 (s, 1H, OH), 3.77–4.35 (complex, 6H, CHCO_2 , $\text{OCH}_2\text{CHCH}_2\text{O}$), 6.79–7.35 (complex, 8H, aryl). $^{13}\text{C NMR}$ (75 MHz, CDCl_3) $\delta_{\text{ppm}} = 18.25$ (C-12), 24.61 (C-9, C-10), 30.07 (C-8), 41.97 (C-11), 46.29 (C-7), 68.01 (C-16), 68.89 (C-17), 70.04 (C-18), 117.20 (C-26), 121.53 (C-24), 122.69 (C-22), 127.92 (C-25), 128.78 (C-1, C-5), 129.36 (C-2, C-4),

4.4.13. *(E)*-2-hydroxy-3-(2-methoxy-4-(prop-1-enyl)phenoxy)propyl 2-(4-isobutylphenyl) propanoate (**1m**)

This compound was obtained as a yellow oil using column chromatography on silica gel (EtOAc:*n*-hexane, 1:10); Yield: 3.41 g, 80%; R_f = 0.29 (EtOAc:*n*-hexane, 1:3); IR (liquid film) ν_{\max} cm^{-1} = 3458 (O–H, Stretch.), 3082 (sp^2 C–H, Stretch.), 2989 (sp^3 C–H, Stretch.), 1749 (C=O, Stretch.), 1463 (aromatic C=C, Stretch.), 1403 (sp^3 C–H, Bend.), 1280 (Ar–O, Stretch.), 1150 (C–O, Stretch.), 870 (sp^2 C–H, Bend.). ^1H NMR (300 MHz, CDCl_3) δ_{ppm} = 0.75 (d, J = 5.7 Hz, 6H, $(\text{CH}_3)_2\text{CHCH}_2$), 1.35 (d, J = 6.6 Hz, 3H, CH_3CHCO_2), 1.74–1.75 (complex, 4H, $(\text{CH}_3)_2\text{CHCH}_2$, $\text{CH}_3\text{CH}=\text{}$), 2.31 (d, J = 6.3 Hz, 2H, PhCH_2), 3.51–4.12 (complex, 10H, CHCO_2 , $\text{OCH}_2\text{CHCH}_2\text{O}$, OCH_3 , OH), 5.95–6.03 (m, 1H, $\text{CH}_3\text{CH}=\text{CHPh}$), 6.18–6.23 (m, 1H, $\text{CH}_3\text{CH}=\text{CHPh}$), 6.57–6.74 (complex, 3H, aryl), 6.92 (d, J = 6.0 Hz, 2H, aryl), 7.05 (d, J = 6.6 Hz, 2H, aryl). ^{13}C NMR (75 MHz, CDCl_3) δ_{ppm} = 17.25 (C-12), 19.59 (C-30), 23.39 (C-9, C-10), 31.30 (C-8), 40.97 (C-11), 45.61 (C-7), 57.02 (C-27), 68.12 (C-16), 69.02 (C-17), 71.34 (C-18), 113.15 (C-23), 116.39 (C-26), 119.62 (C-25), 124.57 (C-29), 128.03 (C-24), 128.96 (C-1, C-5), 129.84 (C-2, C-4), 131.89 (C-28), 133.06 (C-6), 140.39 (C-3), 147.38 (C-21), 152.05 (C-22), 175.45 (C-13). MS (EI): m/z (%) = 426.24 (26.7) [M^+]. Anal. Calcd for $\text{C}_{26}\text{H}_{34}\text{O}_5$: C, 73.21; H, 8.03. Found: C, 73.38; H, 8.17.

4.4.14. 2-hydroxy-3-(*p*-tolylloxy)propyl 2-(4-isobutylphenyl)propanoate (**1n**)

This compound was obtained as a yellow oil using column chromatography on silica gel (EtOAc:*n*-hexane, 1:10); Yield: 3.26 g, 88%; R_f = 0.60 (EtOAc:*n*-hexane, 1:3); IR (liquid film) ν_{\max} cm^{-1} = 3458 (O–H, Stretch.), 3070 (sp^2 C–H, Stretch.), 2985 (sp^3 C–H, Stretch.), 1749 (C=O, Stretch.), 1461 (aromatic C=C, Stretch.), 1416 (sp^3 C–H, Bend.), 1278 (Ar–O, Stretch.), 1157 (C–O, Stretch.), 880 (sp^2 C–H, Bend.). ^1H NMR (300 MHz, CDCl_3) δ_{ppm} = 1.01 (br s, 6H, $(\text{CH}_3)_2\text{CHCH}_2$), 1.60 (br s, 3H, CH_3CHCO_2), 1.94 (br s, 1H, $(\text{CH}_3)_2\text{CHCH}_2$), 2.38 (s, 3H, CH_3Ph), 2.53 (br s, 2H, PhCH_2), 3.48 (s, 1H, OH), 3.85–4.35 (complex, 6H, CHCO_2 , $\text{OCH}_2\text{CHCH}_2\text{O}$), 6.83–7.31 (complex, 8H, aryl). ^{13}C NMR (75 MHz, CDCl_3) δ_{ppm} = 17.64 (C-12), 23.38 (C-9, C-10), 24.82 (C-27), 28.88 (C-8), 41.27 (C-11), 45.91 (C-7), 67.83 (C-16), 69.26 (C-17), 70.72 (C-18), 115.39 (C-22, C-26), 128.39 (C-1, C-5), 129.79 (C-2, C-4), 130.41 (C-23, C-25), 131.56 (C-24), 133.30 (C-6), 139.35 (C-3), 155.51 (C-21), 175.69 (C-13). MS (EI): m/z (%) = 370.21 (23.8) [M^+]. Anal. Calcd for $\text{C}_{23}\text{H}_{30}\text{O}_4$: C, 74.56; H, 8.16. Found: C, 74.40; H, 8.02.

4.4.15. 3-(4-allyl-2-methoxyphenoxy)-2-hydroxypropyl 2-(4-isobutylphenyl)propanoate (**1o**)

This compound was obtained as a yellow oil using column chromatography on silica gel (EtOAc:*n*-hexane, 1:10); Yield: 3.92 g, 92%; R_f = 0.40 (EtOAc:*n*-hexane, 1:3); IR (liquid film) ν_{\max} cm^{-1} = 3496 (O–H, Stretch.), 3075 (sp^2 C–H, Stretch.), 2960 (sp^3 C–H, Stretch.), 1738 (C=O, Stretch.), 1480 (aromatic C=C, Stretch.), 1407 (sp^3 C–H, Bend.), 1266 (Ar–O, Stretch.), 1165 (C–O, Stretch.), 889 (sp^2 C–H, Bend.). ^1H NMR (300 MHz, CDCl_3) δ_{ppm} = 0.77 (br s, 6H, $(\text{CH}_3)_2\text{CHCH}_2$), 1.35 (d, J = 6.0 Hz, 3H, CH_3CHCO_2), 1.73 (br s, 2H, OH,

(CH₃)₂CHCH₂), 2.31 (br s, 2H, PhCH₂), 3.22–4.13 (complex, 11H, CHCO₂, OCH₂CHCH₂O, OCH₃, =CHCH₂), 4.93-
Journal Pre-proofs DCl₃)

δ_{ppm} = 16.70 (C-12), 23.48 (C-9, C-10), 31.18 (C-8), 42.11 (C-11), 46.53 (C-7), 48.86 (C-28), 57.12 (C-27), 68.08 (C-16), 68.95 (C-17), 71.61 (C-18), 114.70 (C-23), 116.77 (C-26), 118.83 (C-30), 123.28 (C-25), 128.30 (C-1, C-5), 129.68 (C-2, C-4), 131.53 (C-24), 133.61 (C-6), 137.74 (C-29), 140.68 (C-3), 144.51 (C-21), 150.71 (C-22), 174.61 (C-13). MS (EI): m/z (%) = 426.24 (27.2) [M⁺]. Anal. Calcd for C₂₆H₃₄O₅: C, 73.21; H, 8.03. Found: C, 73.04; H, 7.89.

Acknowledgments

The authors wish to thank Shiraz University of Technology research council for partial support of this work. The authors are thankful from the High Performance Computing research laboratory of Institute for Research in Fundamental Sciences (IPM).

Declaration of Competing Interest

The authors have declared no conflict of interest.

Appendix A. Supplementary data

Supplementary data to this article can be found online at <https://doi.org/10.1016/j.bioorg.?????????>

References and notes

- [1] C. Patrono, B. Rocca, Nonsteroidal antiinflammatory drugs: Past, present and future, *Pharmacol. Res.* 59 (2009) 285–289. <https://doi.org/10.1016/j.phrs.2009.01.011>.
- [2] A.S. Mehanna, NSAIDs: Chemistry and pharmacological actions, *Am. J. Pharm. Educ.* 67 (2003) 1–7. <https://doi.org/10.5688/aj670263>.
- [3] S. Winiwarter, H.J. Roth, The top ten NSAIDs: A molecular modelling study, *Pharm. Acta Helv.* 68 (1994) 181–189. [https://doi.org/10.1016/0031-6865\(94\)90041-8](https://doi.org/10.1016/0031-6865(94)90041-8).
- [4] M. Manrique-Moreno, P. Garidel, M. Suwalsky, J. Howe, K. Brandenburg, The membrane-activity of ibuprofen, diclofenac, and naproxen: A physico-chemical study with lecithin phospholipids, *Biochim. Biophys. Acta, Biomembr.* 1788 (2009) 1296–1303. <https://doi.org/10.1016/j.bbamem.2009.01.016>.
- [5] M. Manrique-Moreno, J. Howe, M. Suwalsky, P. Garidel, K. Brandenburg, Physicochemical interaction study of non-steroidal anti-inflammatory drugs with dimyristoylphosphatidylethanolamine liposomes, *Lett. Drug Des. Discovery* 7 (2010) 50–56. <https://doi.org/10.2174/157018010789869280>.

erythrocytes and molecular models of eukaryotic membranes, *Biochim. Biophys. Acta, Biomembr.* 1838 (2014) 266–277. <https://doi.org/10.1016/j.bbamem.2013.08.003>.

[7] M. Manrique-Moreno, M. Suwalsky, F. Villena, P. Garidel, Effects of the nonsteroidal anti-inflammatory drug naproxen on human erythrocytes and on cell membrane molecular models, *Biophys. Chem.* 147 (2010) 53–58. <https://doi.org/10.1016/j.bpc.2009.12.010>.

[8] M. Manrique-Moreno, F. Villena, C.P. Sotomayor, A.M. Edwards, M.A. Muñoz, P. Garidel, M. Suwalsky, Human cells and cell membrane molecular models are affected in vitro by the nonsteroidal anti-inflammatory drug ibuprofen, *Biochim. Biophys. Acta, Biomembr.* 1808 (2011) 2656–2664. <https://doi.org/10.1016/j.bbamem.2011.07.005>.

[9] M. Suwalsky, M. Manrique, F. Villena, C.P. Sotomayor, Structural effects in vitro of the anti-inflammatory drug diclofenac on human erythrocytes and molecular models of cell membranes, *Biophys. Chem.* 141 (2009) 34–40. <https://doi.org/10.1016/j.bpc.2008.12.010>.

[10] M. Suwalsky, M. Manrique-Moreno, J. Howe, K. Brandenburg, F. Villena, Molecular interactions of mefenamic acid with lipid bilayers and red blood cells, *J. Braz. Chem. Soc.* 22 (2011) 2243–2249. <http://dx.doi.org/10.1590/S0103-50532011001200002>.

[11] C. Pereira-Leite, C. Nunes, S. Reis, Interaction of nonsteroidal anti-inflammatory drugs with membranes: In vitro assessment and relevance for their biological actions, *Prog. Lipid Res.* 52 (2013) 571–584. <https://doi.org/10.1016/j.plipres.2013.08.003>.

[12] S. Tavolari, A. Munarini, G. Storci, S. Laufer, P. Chieco, T. Guarnieri, The decrease of cell membrane fluidity by the non-steroidal anti-inflammatory drug licofelone inhibits epidermal growth factor receptor signalling and triggers apoptosis in HCA-7 colon cancer cells, *Cancer Lett.* 321 (2012) 187–194. <https://doi.org/10.1016/j.canlet.2012.02.003>.

[13] W. Tomisato, K.-I. Tanaka, T. Katsu, H. Kakuta, K. Sasaki, S. Tsutsumi, T. Hoshino, M. Aburaya, D.L.T. Tsuchiya, K. Suzuki, K. Yokomizo, T. Mizushima, Membrane permeabilization by non-steroidal anti-inflammatory drugs, *Biochem. Biophys. Res. Commun.* 323 (2004) 1032–1039. <https://doi.org/10.1016/j.bbrc.2004.08.205>.

[14] Nonsteroidal anti-inflammatory drug. https://en.wikipedia.org/wiki/Nonsteroidal_anti-inflammatory_drug/, 2020 (accessed 30 September 2020).

[15] A. Kleeman, J. Engel, B. Kutscher, D. Reichert, *Pharmaceutical Substances*, 3rd ed., Thieme, Stuttgart, 1999.

[16] A. Burke, E. Smyth, G.A. Fitzgerald, Analgesic-antipyretic and anti-inflammatory agents: Pharmacotherapy of gout, in: L.L. Brunton (Ed.), *Goodman & Gilman's Manual of Pharmacology and Therapeutics*, McGraw-Hill, New York, 2008, pp. 428–461.

[17] R. Polisson, Nonsteroidal anti-inflammatory drugs: Practical and theoretical considerations in their selection, *Am. J. Med.* 100 (1996) 31S–36S. [https://doi.org/10.1016/S0002-9343\(97\)89544-7](https://doi.org/10.1016/S0002-9343(97)89544-7).

[19] J.R. Vane, R.M. Botting, Anti-inflammatory drugs and their mechanism of action, *Inflamm. Res.* 47 (1998) 78–87. <https://doi.org/10.1007/s000110050284>.

[20] S. Kawai, F. Kojima, N. Kusunoki, Recent advances in nonsteroidal anti-inflammatory drugs, *Allergol. Int.* 54 (2005) 209–215. <https://doi.org/10.2332/allergolint.54.209>.

[21] W.F. Kean, W.W. Buchanan, The use of NSAIDs in rheumatic disorders 2005: A global perspective, *Inflammopharmacology* 13 (2005) 343–370. <https://doi.org/10.1163/156856005774415565>.

[22] K. Shah, J.K. Gupta, N.S. Chauhan, N. Upmanyu, S.K. Shrivastava, P. Mishra, *Open Med. Chem. J.* 11 (2017) 146–195. <https://doi.org/10.2174/1874104501711010146>.

[23] G.M. Nazeruddin, S.B. Suryawanshi, Synthesis of novel mutual prodrugs by coupling of ibuprofen (NSAID) with sulfa drugs, *J. Chem. Pharm. Res.* 2 (2010) 508–512.

[24] X. Zhao, D. Chen, P. Gao, P. Ding, K. Li, Synthesis of ibuprofen eugenol ester and its microemulsion formulation for parenteral delivery, *Chem. Pharm. Bull.* 53 (2005) 1246–1250. <https://doi.org/10.1248/cpb.53.1246>.

[25] V.K. Redasani, S.B. Bari, Synthesis and evaluation of mutual prodrugs of ibuprofen with menthol, thymol and eugenol, *Eur. J. Med. Chem.* 56 (2012) 134–138. <https://doi.org/10.1016/j.ejmech.2012.08.030>.

[26] A.Z. Abdel-Azeem, A.A. Abdel-Hafez, G. El-Karamany, H.H. Farag, Chlorzoxazone esters of some non-steroidal anti-inflammatory (NSAI) carboxylic acids as mutual prodrugs: Design, synthesis, pharmacological investigations and docking studies, *Bioorg. Med. Chem.* 17 (2009) 3665–3670. <http://dx.doi.org/10.1016/j.bmc.2009.03.065>.

[27] T.A. Fadl, F.A. Omar, Paracetamol (acetaminophen) esters of some non-steroidal anti-inflammatory carboxylic acids as mutual prodrugs with improved therapeutic index, *Inflammopharmacology* 6 (1998) 143–157. <http://dx.doi.org/10.1007/s10787-998-0031-3>.

[28] Z. Yang, Y. Zhichao, Z. Hongli, Novel ibuprofen medoxomil prodrug: Design, synthesis and in vitro stability evaluation, *J. Chem. Pharm. Res.* 6 (2014) 2339–2342.

[29] V. Cioli, S. Putzolu, V. Rossi, C. Corradino, A toxicological and pharmacological study of ibuprofen guaiacol ester (AF 2259) in the rat, *Toxicol. Appl. Pharmacol.* 54 (1980) 332–339. [http://dx.doi.org/10.1016/0041-008x\(80\)90203-3](http://dx.doi.org/10.1016/0041-008x(80)90203-3).

[30] F.A. Omar, Cyclic amide derivatives as potential prodrugs. Synthesis and evaluation of N-hydroxymethylphthalimide esters of some nonsteroidal anti-inflammatory carboxylic acid drugs, *Eur. J. Med. Chem.* 31 (1998) 123–131. [http://dx.doi.org/10.1016/S0223-5234\(98\)80037-8](http://dx.doi.org/10.1016/S0223-5234(98)80037-8).

[31] Z. Huang, C.A. Velázquez, K.R. Abdellatif, M.A. Chowdhury, J.A. Reisz, J.F. DuMond, S.B. King, E.E. Knaus, Ethanesulfohydroxamic acid ester prodrugs of nonsteroidal anti-inflammatory drugs (NSAIDs): Synthesis, nitric oxide and nitroxyl release, cyclooxygenase inhibition, anti-inflammatory, and

- [32] F.Z. Abu Zanat, A.M. Qandil, B.M. Tashtoush, A promising codrug of nicotinic acid and ibuprofen for managing dyslipidemia. I: Synthesis and in vitro evaluation, *Drug Dev. Ind. Pharm.* 37 (2011) 1090–1099. <http://dx.doi.org/10.3109/03639045.2011.560155>.
- [33] A.R. Katritzky, D. Jishkariani, T. Narindoshvili, Convenient synthesis of ibuprofen and naproxen aminoacyl, dipeptidoyl and ester derivatives, *Chem. Biol. Drug Des.* 73 (2009) 618–626. <http://dx.doi.org/10.1111/j.1747-0285.2009.00811.x>.
- [34] M.S. Khan, R.M. Khan, Synthesis and biological evaluation of glycolamide esters as potential prodrugs of some non-steroidal anti-inflammatory drugs, *Indian J. Chem.* 41B (2002) 2172–2175.
- [35] N. Mehta, S. Aggarwal, S. Thareja, P. Malla, M. Misra, T.R. Bhardwaj, M. Kumar, Synthesis, pharmacological and toxicological evaluation of amide derivatives of ibuprofen, *Int. J. Chemtech Res.* 2 (2010) 233–235.
- [36] A.A. Lohade, K.P. Jain, K.R. Iyer, Parallel combinatorial synthesis and in vitro evaluation of ester and amide prodrugs of flurbiprofen, ibuprofen and ketoprofen, *Ind. J. Pharma. Edu. Res.* 43 (2009) 140–149.
- [37] M. Babazadeh, Design, synthesis and in vitro evaluation of vinyl ether type polymeric prodrugs of ibuprofen, ketoprofen and naproxen, *Int. J. Pharm.* 356 (2008) 167–173. <http://dx.doi.org/10.1016/j.ijpharm.2008.01.003>.
- [38] B. Mizrahi, A.J. Domb, Anhydride prodrug of ibuprofen and acrylic polymers, *AAPS PharmSciTech* 10 (2009) 453–458. <http://dx.doi.org/10.1208/s12249-009-9228-z>.
- [39] H. Deng, J. Song, A.K. Elom, J. Xu, Z. Fan, C. Zheng, Y. Xing, K. Deng, 2016. Synthesis and controlled release behavior of biodegradable polymers with pendant ibuprofen group, *Int. J. Polym. Sci.* 2016, 5861419. <http://dx.doi.org/10.1155/2016/5861419>.
- [40] W. Xu, K.B. Thapa, Q. Ju, Z. Fang, W. Huang, Heterogeneous catalysts based on mesoporous metal–organic frameworks, *Coordin. Chem. Rev.* 373 (2018) 199–232. <https://doi.org/10.1016/j.ccr.2017.10.014>.
- [41] U. Díaz, M. Boronat, A. Corma, Hybrid organic–inorganic structured materials as single-site heterogeneous catalysts, *Proc. R. Soc. (A)* 468 (2012) 1927–1954. <https://doi.org/10.1098/rspa.2012.0066>.
- [42] E.L. Margelefsky, R.K. Zeidan, M.E. Davis, Cooperative catalysis by silica-supported organic functional groups, *Chem. Soc. Rev.* 37 (2008) 1118–1126. <https://doi.org/10.1039/B710334B>.
- [43] M.A. Zolfigol, Silica sulfuric acid/ NaNO_2 as a novel heterogeneous system for production of thionitrites and disulfides under mild conditions, *Tetrahedron* 57 (2001) 9509–9511. [https://doi.org/10.1016/S0040-4020\(01\)00960-7](https://doi.org/10.1016/S0040-4020(01)00960-7).
- [44] P. Wasserscheid, T. Welton, *Ionic Liquids in Synthesis*, Wiley-VCH Verlag GmbH & Co. KGaA, Weinheim, 2002.

j.apcata.2012.08.007.

[46] H. Li, P.S. Bhadury, B. Song, S. Yang, Immobilized functional ionic liquids: efficient, green, and reusable catalysts, *RSC Adv.* 2 (2012) 12525–12551. <https://doi.org/10.1039/c2ra21310a>.

[47] M.M.A. Pereira, Immobilized ionic liquids in organic chemistry, *Curr. Org. Chem.* 16 (2012) 1680–1710, <https://doi.org/10.2174/138527212800840919>.

[48] J.M. Xu, C. Qian, B.K. Liu, Q. Wu, X.F. Lin, A fast and highly efficient protocol for Michael addition of N-heterocycles to α,β -unsaturated compound using basic ionic liquid [bmIm]OH as catalyst and green solvent, *Tetrahedron* 63 (2007) 986–990. <https://doi.org/10.1016/j.tet.2006.11.013>.

[49] R. Bushra, N. Aslam, An overview of clinical pharmacology of ibuprofen, *Oman Med. J.* 25 (2010) 155–1661. <https://doi.org/10.5001/omj.2010.49>.

[50] M.N. Soltani Rad, S. Behrouz, The base-free chemoselective ring opening of epoxides with carboxylic acids using [bmim]Br: A rapid entry into 1,2-diol mono-esters synthesis, *Mol. Divers.* 17 (2011) 9–18, <https://doi.org/10.1007/s11030-012-9412-z>.

[51] D.J. Langford, J.S. Mogil, *Anesthesia and Analgesia in Laboratory Animals*, Elsevier Science, 2008. <https://doi.org/10.1016/B978-0-12-373898-1.X5001-3>.

[52] A.A. Taherian, A. Rashidi Pour, M. Arefi, A. Vafaei, M. Emami Abarghoei, H. Sadeghi, M. Jarrahi, H. Miladi Gorji, Assessment of hydroalcoholic extract of *Thymus Vulgaris* on neurogenic and inflammatory pain in mice, *J. Babol Uni. Med. Sci. (JBUMS)* 7 (2005) 24–29. <http://jbums.org/article-1-2633-en.html>.

[53] D. Dubuisson, S.G. Dennis, The formalin test: A quantitative study of the analgesic effects of morphine, meperidin, and brain stem stimulation in rats and cats, *Pain* 4 (1977) 161–74. [https://doi.org/10.1016/0304-3959\(77\)90130-0](https://doi.org/10.1016/0304-3959(77)90130-0).

[54] A. Tjolsen, O.G. Berge, S. Hunskaar, J.H. Rosland, K. Hole, The formalin test: An evaluation of the method. *Pain* 51 (1992) 5–17. [https://doi.org/10.1016/0304-3959\(92\)90003-t](https://doi.org/10.1016/0304-3959(92)90003-t).

[55] N. Aarhus, Molegro Virtual Docker, version 6.0.0, CLC Bio, 8200, Denmark, 2012.

[56] O. Laneuville, D.K. Breuer, D.L. Dewitt, T. Hla, C.D. Funk, W.L. Smith, Differential inhibition of human prostaglandin endoperoxide H synthases-1 and -2 by nonsteroidal anti-inflammatory drugs, *J. Pharmacol. Exp. Ther.* 271 (1994) 927–934.

[57] M.J. Frisch, G.W. Trucks, H.B. Schlegel, G.E. Scuseria, M.A. Robb, J.R. Cheeseman et al., *Gaussian 09*, Revision A.01 Gaussian, Inc., Wallingford CT, 2009.

[58] G. Marcou, D. Rognan, Optimizing fragment and scaffold docking by use of molecular interaction fingerprints, *J. Chem. Inf. Model* 47 (2007) 195–207. <https://doi.org/10.1021/ci600342e>.

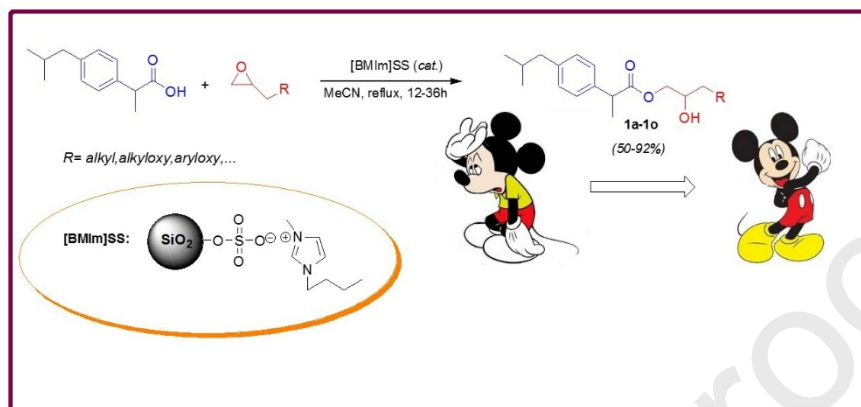
[59] B.J. Orlando, M.J. Lucido, M.G. Malkowski, The structure of ibuprofen bound to cyclooxygenase-2. *J. Struct. Biol.* 189 (2015) 62–66. <https://doi.org/10.2210/pdb4ph9/pdb>.

- [60] K.K. Angajala, S.V. Ramesh Macha, M. Raghavender, M.K. Thupurani, P.J. Pathi, 2016. Synthesis, anti-inflammatory activity of *1,4-dihydropyridin-2(1H)-one* derivatives using click chemistry, *SpringerPlus* 5, 423. <https://doi.org/10.1186/s40064-016-2052-5>.
- [61] R.J. Bienstock, Library Design, Search Methods, and Applications of Fragment-Based Drug Design, American Chemical Society, Washington, 2011.
- [62] C.A. Lipinski, F. Lombardo, B.W. Dominy, P.J. Feeney, Experimental and computational approaches to estimate solubility and permeability in drug discovery and development settings, *Adv. Drug Deliv. Rev.* 46 (2001) 3–26. [https://doi.org/10.1016/S0169-409X\(96\)00423-1](https://doi.org/10.1016/S0169-409X(96)00423-1).
- [63] C.A. Lipinski, Lead- and drug-like compounds: The rule-of five revolution, *Drug Discov. Today* 1 (2004) 337–341. <https://doi.org/10.1016/j.ddtec.2004.11.007>.
- [64] Download Data Warrior V4.7.2. <http://www.openmolecules.org/datawarrior/download.html/>, 2020 (accessed 30 September 2020).

Graphical Abstract

Butyl methyl imidazolium silica sulfate (BMIm)SS: A novel hybrid nano-catalyst for highly efficient synthesis of new 1,2-diol monoesters of ibuprofen as the novel prodrugs of ibuprofen having potent analgesic property

M. N. Soltani Rad, S. Behrouz,* E. Atashbaste, S.-S. Hashemi*



- Novel nano-hybride catalyst (BMIm)SS is prepared and characterized.
- 1,2-diol monoester of IBP is obtained from epoxide and IBP catalyzed by (BMIm)SS.
- 1,2-diol monoesters of IBP show potent analgesic activity using formalin test.
- Docking indicates strong binding of compounds in an active site of COX-2 enzyme.
- *In silico* pharmacokinetic profile was applied to predict potential drug candidate.